Opto-Electronic Advances

Review

2022, Vol. 5, No. 8

DOI: 10.29026/oea.2022.210127

Optical multiplexing techniques and their marriage for on-chip and optical fiber communication: a review

Svetlana Nikolaevna Khonina[1,2]*, Nikolay Lvovich Kazanskiy[1,2], Muhammad Ali Butt[2,3] and Sergei Vladimirovich Karpeev[1,2]

Herein, an attention-grabbing and up-to-date review related to major multiplexing techniques is presented which includes wavelength division multiplexing (WDM), polarization division multiplexing (PDM), space division multiplexing (SDM), mode division multiplexing (MDM) and orbital angular momentum multiplexing (OAMM). Multiplexing is a mechanism by which multiple signals are combined into a shared channel used to showcase the maximum capacity of the optical links. However, it is critical to develop hybrid multiplexing methods to allow enhanced channel numbers. In this review, we have also included hybrid multiplexing techniques such as WDM-PDM, WDM-MDM and PDM-MDM. It is probable to attain *N*×*M* channels by utilizing *N* wavelengths and *M* guided-modes by simply utilizing hybrid WDM-MDM (de)multiplexers. To the best of our knowledge, this review paper is one of its kind which has highlighted the most prominent and recent signs of progress in multiplexing techniques in one place.

Keywords: wavelength division multiplexing; mode division multiplexing; polarization division multiplexing; space-division multiplexing; and hybrid multiplexing

Khonina SN, Kazanskiy NL, Butt MA, Karpeev SV. Optical multiplexing techniques and their marriage for on-chip and optical fiber communication: a review. *Opto-Electron Adv* **5**, 210127 (2022).

Introduction

The relentless pressure for higher data rates ensured the rapid growth of optical components, allowing the terabits (Tbits) of today's data rates to be enjoyed[1,2]. All began with exceptionally lossy fiber optics (hereafter represented as FOs) coupled with a broadband source that could only relay a few Mb/s over a few meters. For half a century, the situation improved dramatically, accomplishing data rates of even Tbit/sec conceivable over a single FO. With the development of external cavity lasers (ECL), it is possible to obtain linewidths below 1 MHz[3,4], Mach-Zehnder modulators (MZM)[5,6] that can simply function at 40 Gb/s and beyond[7], low attenuation dispersion operated FOs, dispersion compensation FOs, optical amplification networks and high-speed detectors that render numerous compensation hardware redundant. Multiplexing is the mechanism by which multiple signals are merged into a shared channel used to tap the maximum volume of the optical links[8]. Multiplexing has traditionally been used to share the medium's inadequate bandwidth (hereafter abbreviated as BW) between multiple transmitters, but it is all about maximum

[1]IPSI RAS-Branch of the FSRC "Crystallography and Photonics" RAS, Samara 443001, Russia; [2]Samara National Research University, Samara 443086, Russia; [3]Warsaw University of Technology, Institute of Microelectronics and Optoelectronics, Koszykowa 75, Warszawa 00-662, Poland.
*Correspondence: SN Khonina, E-mail: khonina@ipsiras.ru

Received: 13 October 2021; Accepted: 12 December 2021; Published online: 15 July 2022

usage of the immense available BW for optical networks.

This is where wavelength division multiplexing (WDM) comes in where numerous channels are multiplexed into a single FO. WDM was implemented as an advance in delivering high volume data broadcast by letting various wavelength channels be concurrently transmitted in a particular FO[9]. Polarization-division-multiplexing (PDM) is one more distinguished strategy to increase data broadcast ability with two polarized channels[10]. In recent times, mode-division multiplexing (MDM) has appeared as a prospective method to upturn the data broadcast size by using numerous spatial guided-modes in multimode waveguides (WGs), which can increase multi-fold optical link volume by employing merely a single wavelength source[11]. MDM tends to be highly appealing for imminent network-on-chip computing because there is no need for an array of precise wavelength lasers like WDM networks. Hybrid multiplexing methods, for instance, MDM-WDM[12] and MDM-PDM[13], have also been introduced. MDM communication has been established with several modes in Si photonic integrated circuits (PICs), in which each mode signified a distinct information channel[14–16]. Numerous constructions, for example, multimode interferometers (MMIs)[17], asymmetric directional couplers (ADCs)[18] and adiabatic mode-evolution couplers[19] among others, have been introduced as PICs MDMs.

Optical multiplexing is an imperative topic and intense research is carried out every year throughout the world. Several research articles based on different multiplexing techniques, for example, WDM, MDM, SDM and PDM among others are published on regular basis. Figure 1 depicts the number of publications on multiplexing topics published in 2000-2020 indexed in the Scopus database. In the year 2020, we can see a significant decrease in the number of publications which can be attributable to the inadequate research activities during COVID-19. In the Image Processing Systems Institute of the Russian Academy of Science, we have fabricated several diffractive optical elements for the realization of MDM in free-space[20,21] and in FO[22,23]. Based on our experience in this vast field, we have tried our best to review recent advancements in the world of multiplexing. The topics covered in this review are WDM, PDM, SDM, MDM, OAMM and three hybrid techniques such as WDM-PDM, WDM-MDM and PDM-MDM. Only the most prominent works are highlighted and cited in this paper.

Over the past 4 decades, several industrial advances have endorsed the FO volume to upsurge by about 10 times every four years as seen in Fig. 2. Until now, broadcast infrastructure has been able to continue with the persistent rapid evolution of Internet protocol traffic. The cost of sending additional data was still practicable, primarily because more data was transmitted over the same FO by customizing the FO end apparatus. However, a growing number of FOs will surpass their performance in actual networks over the next decade or

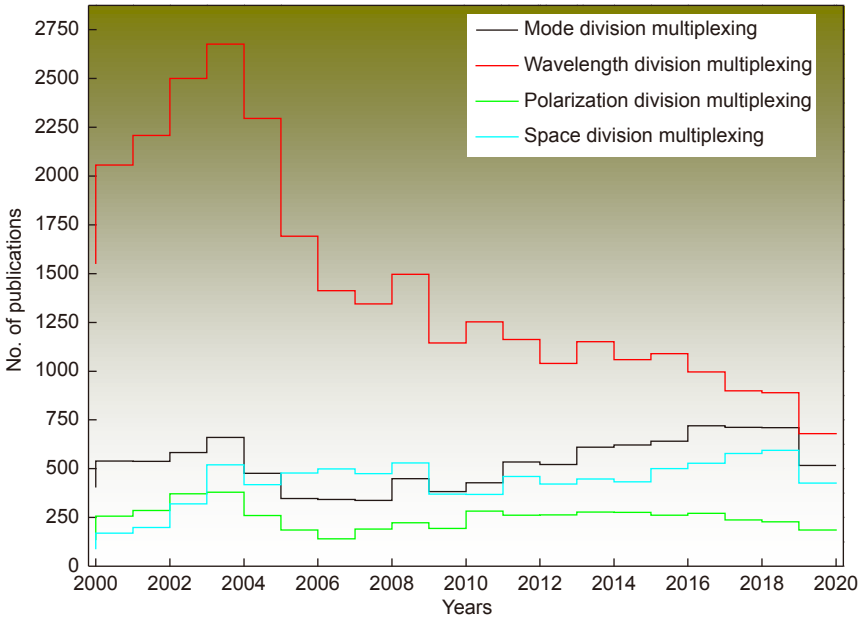

Fig. 1 | The number of research papers associated with different multiplexing techniques indexed in the Scopus database.

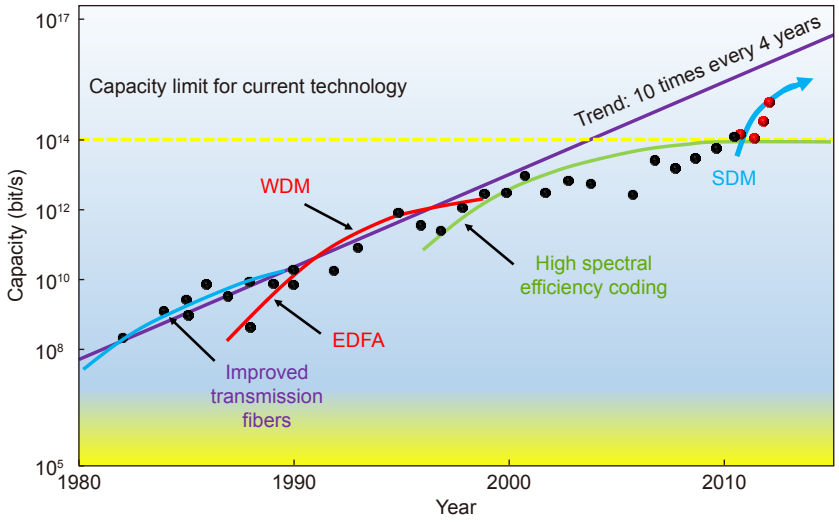

Fig. 2 | The advancement of transmission volume in FOs established by the state-of-the-art laboratory.

so[24]. Besides, this constraint of FO volume is not explicit to a particular modulation scheme; rather it is necessary to derive from a basic expansion of the Shannon volume limit for a nonlinear FO channel under reasonably general beliefs[25]. The drawback is that at spectral efficiency of ~10 bit/s/Hz, a typical single-mode fiber (SMF) will hold no more than 100 Tbit/s of data equal to the C and L amplification wavelength regime of an erbium-doped fiber amplifier.

The paper is organized in the following manner: At first, the recent advances in the major multiplexing techniques such as wavelength division multiplexing (WDM), polarization division multiplexing (PDM), space division multiplexing (SDM), mode division multiplexing (MDM) and orbital angular momentum multiplexing (OAMM) are discussed and it is revealed that how multiplexing is vital to boost the capacity of the optical link. It is important to progress hybrid multiplexing techniques to permit higher channel numbers. Afterwards, hybrid multiplexing techniques such as WDM-PDM, WDM-MDM and PDM-MDM are discussed and recent developments in this topic have been presented. The authors of this paper are working on this topic for more than 3 decades. In the end, a section related to the authors' contribution to the multiplexing field is presented followed by the concluding remarks.

Wavelength division multiplexing (WDM)

Network BW is like the wardrobe in your home, you will never get plenty of it. And the data flow is making the demand for communication volume expand faster than the teenager's wardrobe with a no-limit credit card. Short email messages are being switched to BW-hogging animated graphics. Data, video, and voice signal broadcast networks that had sufficient space just a few years ago. Now, the telecom sector wants out of the box approaches to fulfill the never-ending need for BW. WDM technology enables optical channels to be concurrently transmitted via a single FO at different wavelengths, which is a valuable source of making full usage of the low-loss characteristics of FOs over a large wavelength range. The term WDM is generally used for an optical carrier (usually defined as wavelength), while frequency-division multiplexing (FDM) is usually used for a radio carrier (which is most frequently termed as a frequency). Meanwhile, wavelength and frequency are connected by a directly inverse correlation, the two expressions represent a similar notion. The use of the orthogonal-frequency-division-multiplexing (OFDM) format for passive optical networks has piqued researchers' interest recently. OFDM signals have high spectral efficiency, a high tolerance for fiber chromatic dispersion, and a great degree of flexibility when it comes to multiple service provisioning and dynamic BW allocation[26–29].

The theory was first proposed by Delange in 1970[30], but it was in the mid-1977 that basic research on WDM technology had only begun. The research focused on practical implementations for communication networks[31,32]. Since then, exploration has accelerated, along with histrionic development in FOs, light sources and photodetectors (PDs). In particular, optical multiplexer/demultiplexers (MUX/DEMUX), which are the main elements in the WDM broadcast networks, are at present among the most common R&D methods. A

WDM network employs a MUX to connect the signals at the transmitter, and a DEMUX to break them apart at the receiver. It is probable to provide a network that does this concurrently and can act as an optical add-drop MUX with the proper type of FO. Etalons, thin-film-coated optical glass-based single-frequency Fabry–Pérot interferometers have historically been used as optical filtering devices. Several types of MUX/DEMUX have been suggested and produced for data purposes.

Even though WDM technology is not currently fully grown, it has been increasingly employed in functional networks in some countries. Predictably, this technology will dominate shortly optical communication infrastructure. This is largely owing to the outstanding use of WDM, which is focused on the employment of the broad low-loss spectrum region in FOs. Currently, WDM technology is one of the widespread study and expansion topics and several review articles have already been published[33,34]. The basic configuration of the one-way WDM broadcast is shown in Fig. 3. The benefits of WDM networks are increase in broadcast size per fiber, reduction in network cost, concurrent broadcast of multiple modulation-scheme signals, and service channel expandability after FO implementation. Because of these reasons WDM technology is supposed to be broadly installed in diverse fields of optical communication networks.

Generally, WDM networks are used by telecom enterprises because it facilitates the volume expansion of the network deprived of adding more FOs to the network. It is possible to provide numerous generations of technology expansion in their optical network by employing WDM technology and optical amplifiers without renovating the mainstay network. The volume expansion of the given connection can be achieved by merely improving the MUX and DEMUX designs at the transmitter side and receiver side, respectively. In ref.[35], a white-lighting (WL) and WDM-visible light communication (VLC) network with a free-space distance of more than 20 meters and a lighting distance of 3 meters is validated by an RGB triple-source polarization-multiplexing scheme, broadcast gratings, and a dual convex lens. Integrating four-level pulse amplitude modulation (PAM-4) with a triple source polarization-multiplexing network, the peak broadcast rate is substantially increased to 300 Gb/s. WL is created by multiplexing the RGB lights with two gratings and disjointed by DEMUX via the other two gratings. By assuming a dual-convex diffuser, the WL is spread over 3 meters of free space to deliver general WL illumination (>100 lux). These verified WL and WDM-VLC networks achieve a high broadcast rate with an indoor lighting target. It would open a novel classification for lighting and optical broadcast. The basis of the suggested WL and WDM-VLC network employing broadcast gratings and a tailored diffuser over a 20-meter FSO link with a 3-meter lighting distance is shown in Fig. 4. The images of the experimental setup are also shown in Fig. 4(a), and the detailed experimental results can be found in ref.[35].

A novel design of an integrated WDM receiver chip is manufactured on the SOI platform which is equipped with a 25-channel Si nanowire-AWG[36]. Every channel is incorporated with a Ge-on-Si WG PD. The PDs display a current density of 16.9 mA/cm^2 at −1 V and extraordinary sensitivity of 0.82 A/W at 1.55 μm. Wide BWs of 23 GHz and 29 GHz are attained at 0 and −1 Volt, respectively. Every channel can function at 50 Gb/s with low optical input power even below zero bias resulting in a collective data rate of 1.25 Tb/s. The optical micrographs of the receiver chip are revealed in Fig. 4(b). Eye diagrams of channels 5, 10, 15, 20, and 25 at 40 Gb/s and 50 Gb/s were obtained from PD currents between 90 and 110 μA, as displayed in Fig. 4(c). The experimental details can be found in ref.[36].

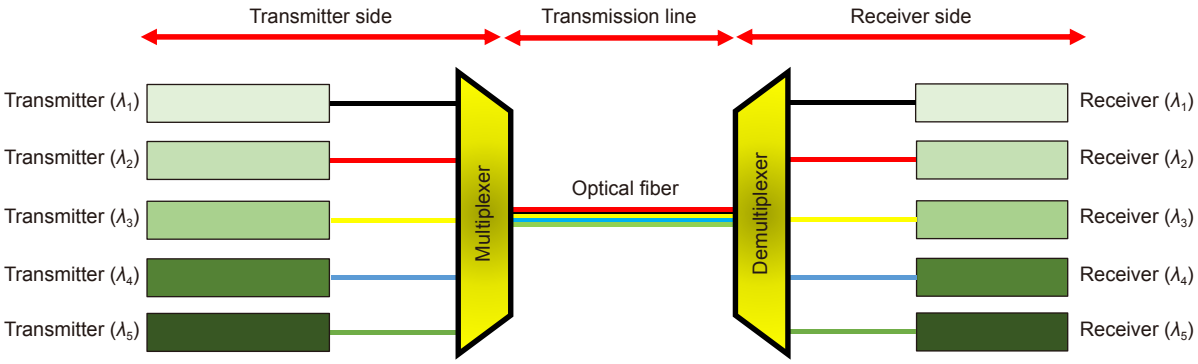

Fig. 3 | Schematic representation of one-directional WDM broadcast.

Polarization division multiplexing (PDM)

Multiplexing is an encouraging solution in reply to the ongoing demand for increased broadcast volume. As the most common and advanced form of multiplexing, WDM has been used successfully for many years. With the growing requirement for BW development, dense WDM networks with a range of laser sources are being utilized, resulting in dense and costly deployment. Besides, it is demonstrated that a typical single-mode FO cannot hold more than 100 Tbit/s data due to its physical limitation[37]. It is also important to introduce new strategies to additionally improve the broadcast BW. The lucrative approach is to multiplex the various aspects of the single-wavelength light carrier such as polarization, referred to as PDM.

A desirable proposal for network operators is to improve the broadcast capability or spectral effectiveness of a current FO network deprived of needing to modify any aspect of the communication hardware or software, so it will dramatically reduce the downtime of the network and decrease the cost of apparatus and connection for network upgrade. One optical method employed to enhance the performance of optical broadcast networks is PDM[38]. The advantage of PDM is that the broadcast volume is multiplied since separate signals can be

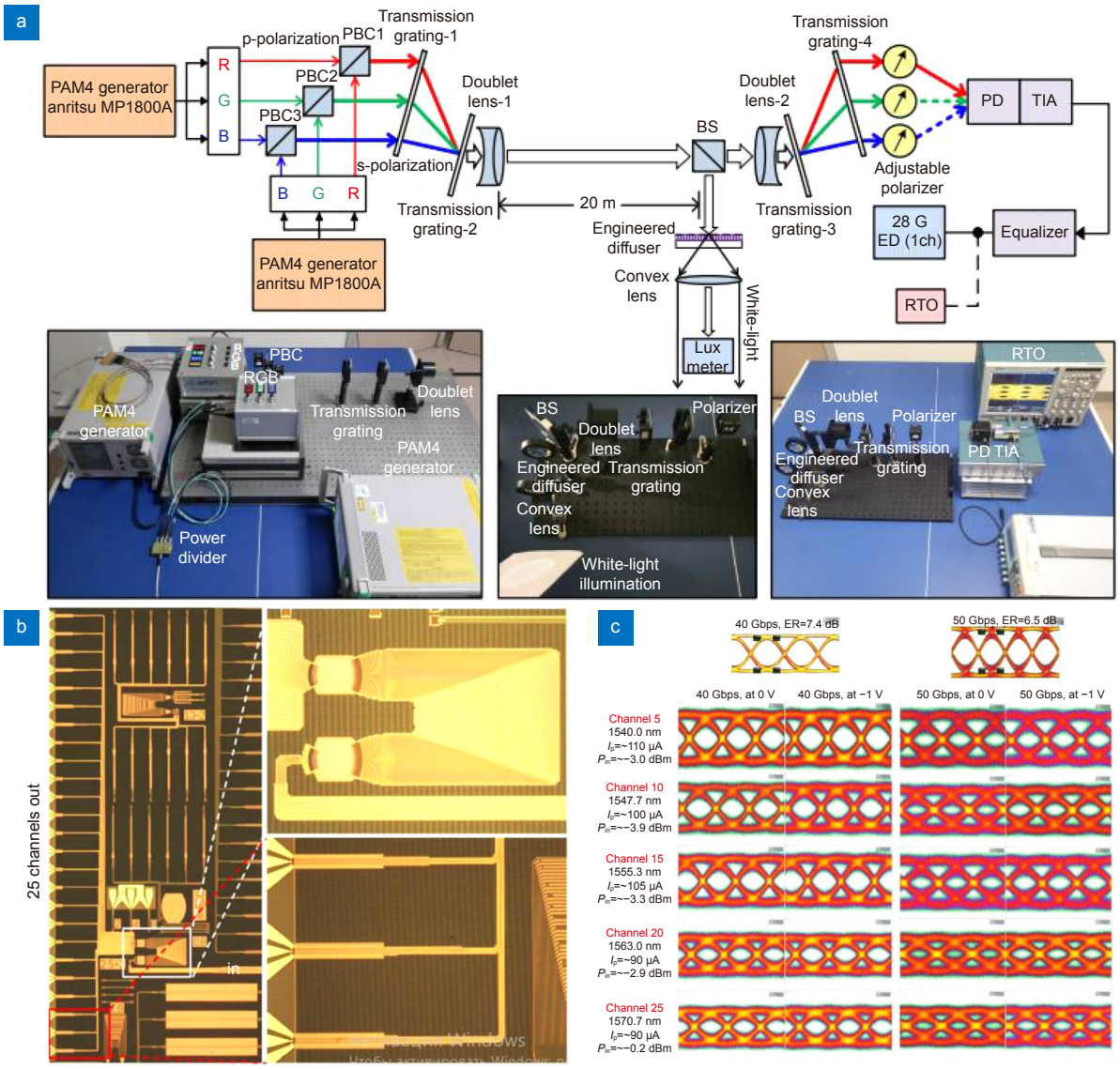

Fig. 4 | (**a**) Graphical illustration of the white-lighting and WDM-VLC network utilizing broadcast gratings and a tailored diffuser over a 20 m FSO link with a 3 m lighting distance. (**b**) Optical micrographs of the WDM receiver chip. (**c**) 40 Gbps and 50 Gpbs eye diagrams of channels 5, 10, 15, 20 and 25 at 0 and –1 V. The modulator eye graphs are also displayed for evaluation. Figure reproduced from: (a) ref.[35], Optical Society of America; (b) ref.[36], Optica Publishing Group, under the Optica Open Access Publishing Agreement.

distributed over orthogonal positions of polarization of the same light[39]. The two polarization channels are separated at the receiver end and are independently recognized. Ideally, at each end of the FO link, the operator only needs to install a transceiver and a related polarization MUX/DEMUX, while the residual network is unaffected which includes FOs, repeaters, amplifiers, wavelength MUX/DEMUX, optical add/drop MUX, switching optics and even the network managing software, or with a slight alteration. The spectral performance of the network can be enriched by minimizing the channel wavelength spacing or aggregating the bit rate of the transceiver. In recent times, several schemes are proposed such as monitoring of pilot tones[40,41], multi-level electronic detection[42] and cross-correlation recognition of the two demultiplexed channels[43]. However, this method entails a momentous re-design of the network, and are thus not appropriate for upgrading current networks, although it might be practicable for new networks to be introduced.

Subcarrier multiplexing (SCM) is another method used to improve the BW of optical networks. The SCM technique joins numerous electrical signals having diverse frequencies to be communicated over the same optical light. Passive optical networks (PONs) based on SCM allow multiple consumers to share the optical channel and the related optical apparatuses minimizing the total network cost[44]. In recent years, the commercial disposal of cost-effective electro-optic modulators with wide frequency ranges and strong linearity has encouraged the use of SCM methods with OFDM-based signals[45]. The integration of PDM and SCM strategies opens the potential for optical network volume to be maximized.

PDM is a simple method, requiring two channels with orthogonal polarizations to be combined only by a polarization beam combiner (PBC) as shown in Fig. 5. However, it is not easy to distinguish the two channels at the receiving end with tolerable crosstalk (CT), since the polarization positions of the two channels are no longer linear, and randomly change with time. To isolate those with a polarization beam splitter (PBS), it is conceivable to observe the CT of the two channels in real-time and then make use of the scrutinized data to vigorously regulate the positions of polarization of the two polarization channels. To date, no good method of optical CT tracking has been identified; thus, one must depend on the identified electronic signal in the receiver to display CT. Research has been devoted to designing the MUX, as an elementary functional component, with silicon on insulator (SOI) platform[46,47]. Likewise, much attention has also been paid to designing the other important modules for example data exchange[48], mode filter[49], power splitter[50], and switch[51], among others.

Interest in visible light communication (VLC) has gradually grown, fueled by the dramatic growth of LED technology[52,53]. Widespread usage, cost-efficient high brightness, improved BW compared to other traditional RF-based devices make it the most capable contender for concurrent lighting and communication mainly in particular areas such as hospitals, aircraft, and high-security prerequisite environments, among others. Though, the comparatively poor intrinsic modulation BW of commercially offered LED is the major technological difficulty in the VLC framework. Recently, a VLC network based on PDM is proposed[54]. The polarization feature of visible light carries with it another degree of freedom that can multiply the volume of the broadcast. To obtain PDM, two orthogonal groups of polarizers and incoherent RGB LEDs are introduced. Due to the minimal laboratory parameters, the red LED chip of the RGB LED is used. Moreover, the spectrally effective 16QAM

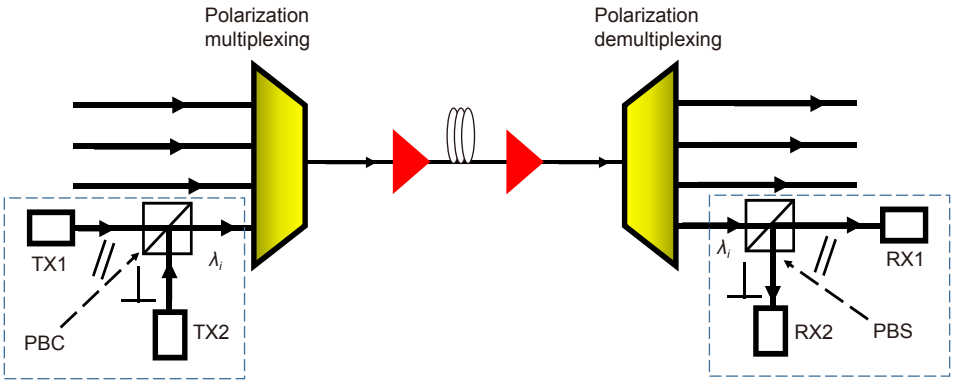

Fig. 5 | Schematic representation of the PDM network.

Nyquist single carrier frequency domain equalization (SC-FDE) is established. However, it was validated on an optical bench, and hence not suitable for CMOS integration. Division-of-focal-plane (DoFP) polarimeters combined with CMOS technology allow dense, polarization imaging networks[55]. The DoFP polarimeters are made up of aluminium nanowire materials and attached to custom CMOS chips. This device includes a complete image processing pipeline that runs at frame rates of 40 f/s and thus allows real-time polarization properties to be derived from the imaged environment. Successful incorporation of high-speed photodiodes into CMOS ICs for a functioning CMOS-compatible optical digital clock delivery is established and electrical recovery network in a 0.35 μm CMOS process. This paper shows the feasibility of low-cost optical-electrical signal conversions at GHz speeds[56].

In ref.[57], a Verilog model of the PDM VLC network is presented. The model is regulated by utilizing the information from manufactured filters and is joint with diode and receiver circuit models. Light is characterized by its three major properties, i.e., wavelength, polarization, and intensity. In this network, the light intensity is used to transport the encrypted data, and polarization to discrete multiple channels. Each input light signal at a diverse polarization angle is modulated to symbolize one digital data channel and joined into one in free space at the source. This incident light is going to form the input to the network. Each data channel has a distinctive polarization angle. In the case of the 2-channel network, the polarization angle of the data channels is 0° and 90°. In the case of the 3-channel network, the data channel polarization angles are 0°, 60° and 120°. Whereas in an event of a 4-channel network, 0°, 45°, 90° and 135° are used as the data channel polarization angles. This combined input light signal is collected by a DoFP polarimeter array which may have 2, 3 or 4 filters depending on the channel design. Each filter from the array will have a polarization angle that matches the polarization angle of one channel of the input light. This work signifies a good starting point to attain improved outcomes for a 4-channel VLC network, plus the usage of channel coding to increase the output. The schematic of the 4-channel VLC network is shown in Fig. 6.

Space division multiplexing (SDM)

Currently, most optical broadcast networks utilize single-mode fibers (SMFs) to transfer data over long distances. More degrees of freedom are accustomed to improving the data rate of SMFs, such as different wavelengths, both polarizations and quadrature amplitude modulation[58]. Technologies for instance coherent receivers and more sophisticated signal processing that can reimburse many of the effects that arise during the broadcast to further improve the data capacity of optical broadcast networks. However, with the latest technologies,

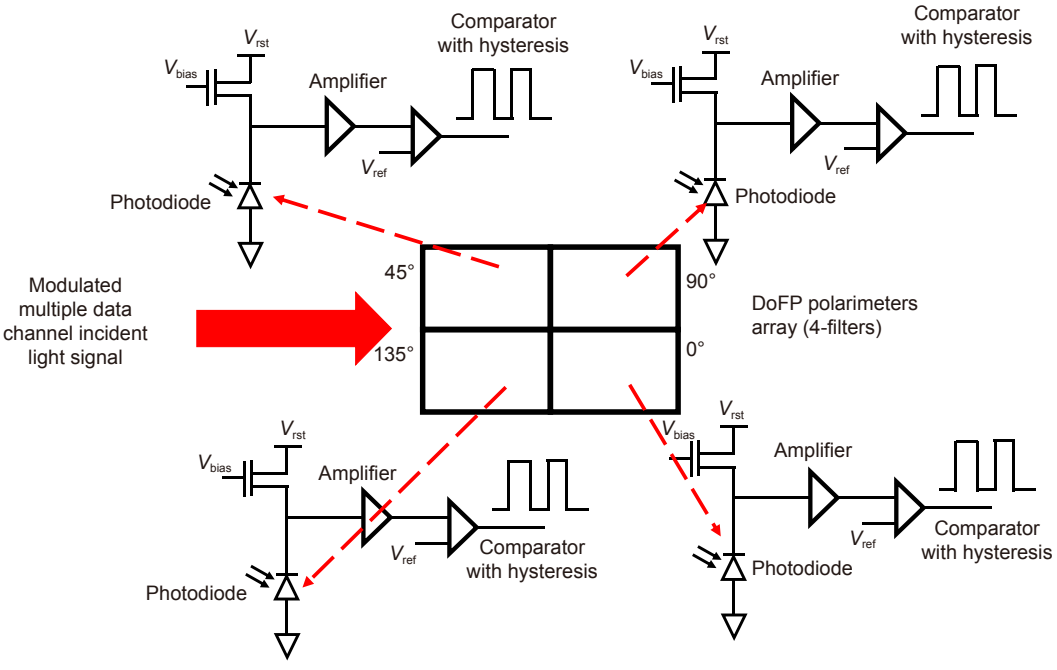

Fig. 6 | 4-channel VLC network. Figure reproduced from ref.[57], SPIE.

the data rates or spectral competence that can be attained in an SMF tends to be constrained by noise and non-linearity with a volume of 100 Tbit/s per fiber or a spectral efficiency of about 10 bit/s/Hz[37]. With a growing request for greater data rates, the last degree of freedom for multiplexing, that is space, has been intensively studied in the last decade as a potential resolution to meet the BW demand.

The schematic representation of the $N \times N$ SDM communication structure is demonstrated in Fig. 7. The signals are primarily produced by N number of transmitters. MDM of the N signals is attained via the spatial-mode multiplexer. Eventually, the signals supported by spatial modes are transferred to the few-mode fiber (FMF). All the modes on the same wavelengths are to be handled as a unit of an SDM super-channel during the broadcast i.e., they are amplified, dropped, and added simultaneously deprived of individual mode processing. After broadcast over FMF, the received signals are then mode DEMUXED by a spatial-mode demultiplexer. Then N coherent receivers detect the demultiplexed signals. The signals are then transformed from an optical-to-electrical domain, electrically sampled with high-speed ADCs, and then analyzed utilizing a DSP module. The MIMO algorithm is employed to compensate for the mode coupling and/or CT in the channel that can be applied at S-MUX/DEMUX or inside the FMF. The channel volume is supposed to be improved by N times as compared to single-mode configuration if the MUX/DEDUX has a unit transfer function with an N-rank equivalent to the number of modes maintained in an SDM FO.

Various parallel spatial channels are employed in SDM to upsurge the data throughput of a broadcast network. Parallel SMF networks can be employed to increase the data rate by the number of utilized FOs to realize SDM as presented in Fig. 8(a). However, with the number of parallel networks, the price and energy ingesting of such parallel networks also surge linearly and there may be attractive methods to realize SDM, where some elements like FOs, amplifiers, transmitters, and receivers can be commonly used between the various spatial channels, reducing the cost/bit. Several distinct methods of implementing SDM with FOs are shown in Fig. 8. Multicore

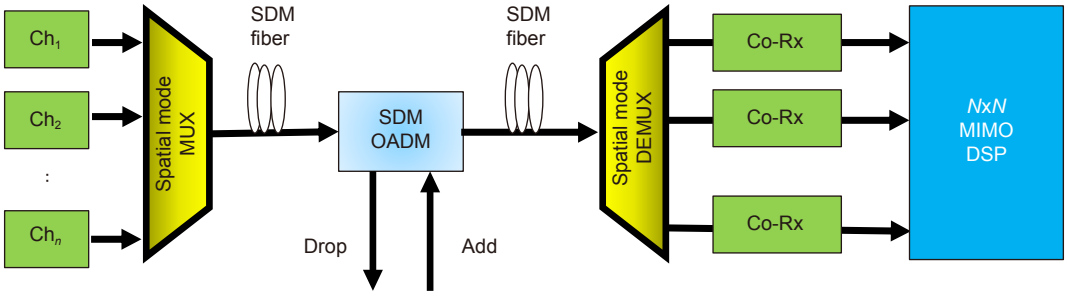

Fig. 7 | The design of an *NxN* SDM communication network using coherent MIMO digital signal processing. Where MUX/DEMUX represents multiplexer/demultiplexer and Co-Rx signifies Coherent receiver.

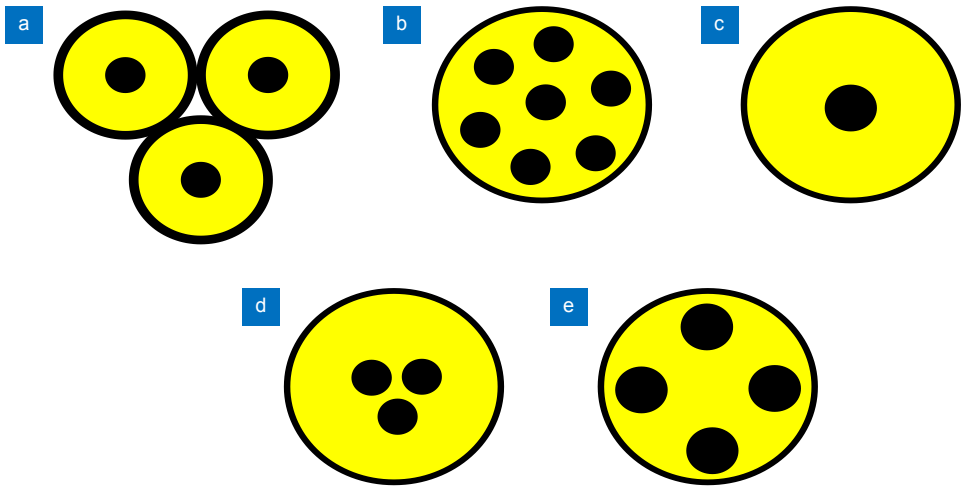

Fig. 8 | Different dissimilarities of FOs for SDM. (**a**) FO bundle, possibly with compact cladding diameter. (**b**) Multicore FO with uncoupled cores. (**c**) Few-mode FO. (**d**) Coupled-core multicore FO. (**e**) Multi-mode-multicore FO, in which each core supports more than one mode.

FOs (MCFs) with uncoupled cores are one rather straightforward way[59]. Each core acts basically as an SMF in such FOs[60]. The CT between cores is low enough not to damage the performance of each channel when the cores are sufficiently separated, see Fig. 8(b). Many low CT FOs and up to 37 cores have been manufactured and broadcast has been demonstrated over long distances[61,62]. Besides, amplifiers have been introduced that can simultaneously amplify all cores[63]. Mode division multiplexing (MDM) is another method for performing SDM where different orthogonal modes of FO are employed as separate spatial channels to transfer data. FMFs are typically used for the MDM method as shown in Fig. 8(c). FMFs are known as multi-mode fibers (MMFs) that can hold few modes, often in the range of 2 –10 modes[64,65]. Coupling between the different FO modes should be considered in MDM. When communicating over longer distances, mode coupling is inevitable. There will be a robust coupling between modes of the same mode group, even for short distances. By employing multiple-input-multiple-output (MIMO) signal processing, mode coupling can be restricted.

Another prospect for SDM is multicore FOs with cores that are adequately close to couple, see Fig. 8(d)[66]. The light travels between the cores in super-modes and acts analogous to FMF. Integration between multicore and FMFs has also been shown in Fig. 8(e). Here, several cores are supported by each core of the multicore FO and the FO can thus reach an enormous number of spatial channels. Several such FOs and their broadcasts have been demonstrated in ref.[67,68]. Besides, SDM can help to address the growing energy consumption of broadcast networks which is in line with the need for higher data speeds[69]. It is more energy efficient to employ multiple spatial channels rather than optimizing the signal-to-noise ratio by increasing the input power into FOs can maximize the data rate in the FO.

Mode division multiplexing (MDM)

Silicon (Si) photonics has been technologically advanced in the last decade as a result many attractive applications are realized on an SOI platform utilizing the complementary metal-oxide-semiconductor (CMOS) fabrication technology[70,71]. Si has a large transparent window covering the near-IR to mid-IR wavelength range, which is critical for achieving low-loss on-chip optical WGs[72,73]. Moreover, it is conceivable to have compact photonic devices owing to the high index contrast between the Si core and the SiO_2 substrate[74,75]. The small footprint helps in decreasing power usage for active Si photonic devices. At present, various Si photonic devices are established with extraordinary performances[76–79]. Most of the time, PICs are typically equipped with merely fundamental mode because higher-order modes are typically very irritating because of the intolerable CT and propagation loss produced due to multimode interference (MMI)[80]. Thus, the optical WGs are typically aimed to be single-mode, such that higher-order modes are cut off. The circumstance is currently evolving with the progress of Si photonics having an exceptional feature of its high refractive index difference. Using a variety of different technologies, several on-chip MDM compatible mode MUXs have been presented[81–85]. In a spot-based approach, most on-chip networks operate and use grating couplers to vertically emit light spots with diverse phases. The intended mode within an FMF can be stimulated by generating the right field pattern above the chip. Different devices have been testified based on the SOI platform[86,87].

Because of their small footprint, low power consumption, and high production output, PICs have demonstrated significant benefits in optical transceivers. For MDM optical interface, multimode chip-to-fiber couplers provide an essential link between PICs and FMF. Chip-based mode MUX/DEMUX and on-chip MDM connectivity have gotten a lot of attention. Several integrated mode converters and multiplexers have been proposed, but only a handful are capable of multimode coupling[83]. The most difficult part is the multimode interface, which serves as a link between the on-chip multimode WG and the FMF. Chip-to-fiber vertical/edge connection typically uses a grating coupler or a spot size coupler. To meet the huge mode field difference between integrated WG and silica fiber in the case of multimode, specific designs must be used. A pair of 2D grating couplers with significant coupling loss and a push-pull solution was presented for exciting 6 linear polarization modes[87]. Later, other multimode grating couplers were constructed with a simpler and more compact construction. While the grating coupler's intrinsic limitation, notably its restricted bandwidth, prevents the application from being compatible with wideband WDM.

Figure 9 displays the dispersion curves of the standard SOI strip WG with a silicon core height of 220 nm[88]. It is well noted that SOI strip WG has extraordinary birefringence and robust mode dispersion. Consequently,

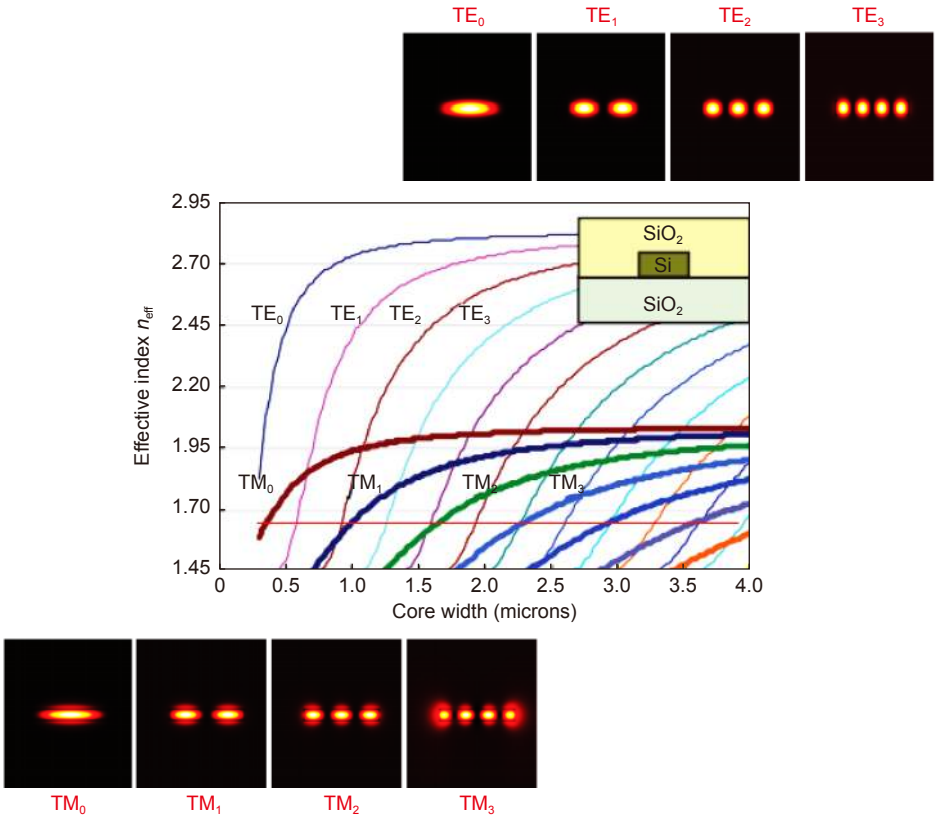

Fig. 9 | Effective refractive indices of the guided modes versus width of the core width. Inset shows the mode shapes of the fundamental and higher-order modes. Figure reproduced with permission from ref.[88], under a Creative Commons Attribution 4.0 International License.

mode-selective modulation with low excess losses and low inter-mode CT can be realized for all the guided modes in a multimode SOI WG even though these guided modes are coincided in space, as displayed in the inset of Fig. 9. This brings the possibility of the use of higher-order modes by incorporating multimode optical WGs in the design of Si photonic devices. Light has a limited range of physical characteristics such as wavelength, polarization, amplitude/phase that can be employed to encrypt data. However, all these encoding methods are approaching their limits and soon the connection speeds will fall far short of demand. There is only one remaining degree of freedom that is still essentially unexplored i.e., "Space". In this way, space is the final destination of FO communication. In MDM, different spatial profiles (i.e., different shapes) known as modes are allocated light beams for different channels. A straightforward scenario will be sending one channel on a laser beam shaped like a circle, one like a square and one like a triangle. The shapes used are more complex in operation and have unique mathematical and physical features. This technique is arguably the most ground-breaking revolution in how data has been transmitted down FOs since at least the 1980s. MDM method offers a

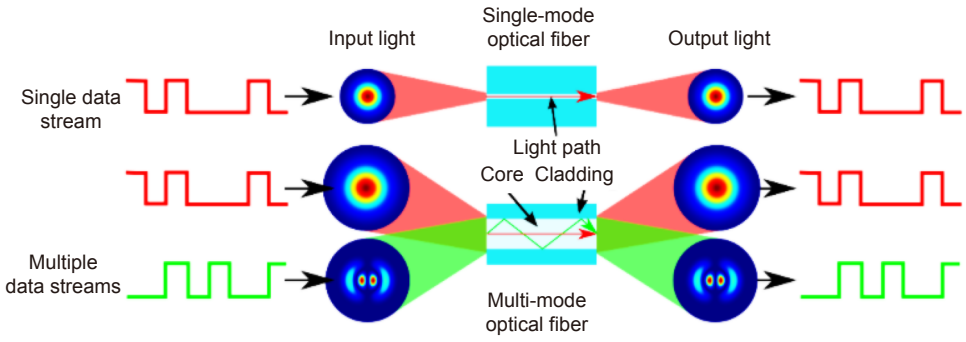

Fig. 10 | The operation principle of MDM. The scheme is adapted from ref.[90].

novel tactic for realizing more channels and augmenting the link volume with a single wavelength carrier[89]. The operation principle of the MDM is shown in Fig. 10.

In ref.[91], a novel scheme of an on-chip two-MDM circuit is proposed by employing tapered directional coupler (DC)-based mode MUX and DEMUX on the SOI platform. The design offers high merits such as low insertion loss of 0.3 dB, low mode CT of < −16 dB, wide BW which is approximately 100 nm. The mode multiplexing testing is performed on the manufactured circuit with non-return-to-zero (NRZ) on-off keying (OOK) signals at 40 Gbit/s. Figure 11(a) displays the manufactured device consisting of a MUX (detail in Fig. 11(b)) at the input side, a multimode data bus WG (750 nm wide), and a DEMUX at the output side. The width of the narrow WG is 355 nm, the wide WG is tapered from 748 nm to 848 nm, and the coupling gap is 100 nm, as presented in Fig. 11(c) and 11(d).

In ref.[92], a compact Si mode (de)MUX with cascaded asymmetrical DCs is verified. A 4-channel mode MUX/DEMUX is considered and comprehended for TM-polarized light. The manufactured device has an excess loss of <1 dB as well as low CT ≤ 23 dB over a wide range of wavelengths. It is possible to add more channels by employing two arrangements of orthogonal-polarization modes (e.g., $2N$=8) multiplexed when preferred. Power splitters split the light from the laser diode into $2N$ channels. As the power of each channel is $1/2N$, an optical amplifier should be added to reimburse for the loss if necessary. The polarization of half of the channels is alternated via a polarization rotator array. As a result, two orthogonally polarized lights are achieved. The $2N$ channels are then linked to the $2N$ optical modulators. These $2N$ channels are eventually merged with a MUX. At the receiver end, multichannel signals can be demultiplexed with a DEMUX which is then collected by a PD array. As it is typically uncommon for PDs to be susceptible to polarization, polarization rotators are added before the PD array to use the same PDs on the chip, which facilitates streamlining the configuration of the chip. Since merely one laser is required and there is no requirement to critically monitor the wavelength, the administration of the hybrid multiplexing network is easy and the cost is supposed to be minimal. The graphical representation of the demonstrated design is displayed in Fig. 11(e).

A unique on-chip information conversion circuit for the MDM signals is proposed by employing two μ-ring resonators (μ-RRs) established mode converters[93]. Single and four wavelengths non-return-to-zero on-off-keying signals at 10 Gb/s passed on diverse modes are managed. The bit error ratio results indicate practical power losses. The graphical representation of the proposed circuit is shown in Fig. 11(f). MDM signals encompassing TE_0 and TE_1 modes transfer into the first μ-RR (μ-RR-1), which achieves the TE_1–TE_0 mode transformation. The configuration of μ-RR-1 is displayed in Fig. 11(g). The drop port and ring bend WGs of μ-RR-1 are designed to be single-mode, whereas through port WG's width is

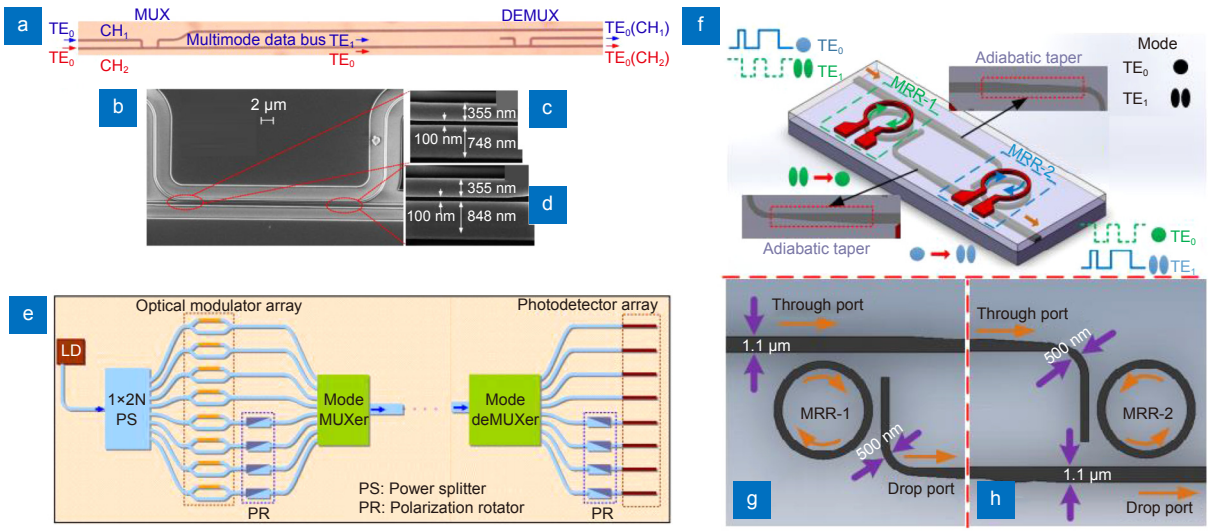

Fig. 11 | (**a**) Manufactured TE_0 and TE_1 mode MUX circuit. (**b**) SEM images of a manufactured TE_0 and TE_1 mode (de)MUX and details of its. (**c**) Input side. (**d**) Output side[91]. (**e**) Graphical representation of a multimode SDM circuit with two polarizations. (**f**) Schematic of the circuit and structures of (**g**) μ-RRs-1, (h) μ-RR-2. Figure reproduced from: (a–d) ref.[91], Optica Publishing Group, under the Optica Open Access Publishing Agreement; (e) ref.[92], Optical Society of America; (f–h) ref.[93], Optica Publishing Group, under the Optica Open Access Publishing Agreement.

precisely tailored to gratify the phase-matching condition in the coupling region between fundamental mode of ring bend WG and TE_1 mode of through port WG. TE_1 mode signal will be transformed into TE_0 mode at the drop port whereas the TE_0 mode signal retains unaffected by propagating through μ-RR-1 at the through the port. Instead, the μ-RR-2 works as a TE_0-TE_1 mode transformer. The assembly of μ-RR-2 is symmetric with μ-RR-1, as displayed in Fig. 11(h).

Orbital angular momentum multiplexing (OAMM)

Due to its potential to provide high-speed wireless transmission, wireless communication employing OAM has recently attracted a lot of attention as an emerging possibility beyond 5G technology. OAM is a physical feature of EM waves in which the propagation path is defined by a helical phase front. Wireless OAMM may effectively boost the transmission rate in a point-to-point link such as wireless backhaul and/or fronthaul since the feature can be exploited to establish numerous separate channels[94,95]. Yan et al. established the viability of OAM multiplexing by reaching 32 Gbps transmission utilizing the 28 GHz frequency in 2014[94] and the 60 GHz band in 2016[96]. Because OAMM is a novel technique, it is critical to test its viability from different viewpoints. In the same way, as multiple-input multiple-output (MIMO) technologies employ multiple antenna elements, this technique does as well. Multiple beams conveying various OAM modes are superimposed using the elements.

Antenna components are linked to phase shifters that rotate $n \times 360^{o}$ to form the beam carrying the OAM mode n (L=n). Figure 12(a) depicts an example of OAM mode 0, 1, and 2 beam generation employing uniform circular arrays (UCAs) with eight antenna components. It's worth noting that for multiple OAM mode generation, it is possible to utilize either a single UCA or multiple UCAs. In the first example, a single UCA transmits superposed beams. Concentric multiple UCAs are employed in the later situation. Separation of OAM-carrying beams can be accomplished in a manner like that used for the generation, with antenna components coupled to phase shifters rotating in different directions. Rotations of $n \times 360^{o}$ are orthogonal to one another if the number of antenna elements is more than $2n$. As a result, the signals of each OAM mode may be isolated from those of mixed OAM modes without aliasing. Figure 12(b) depicts an example of each antenna element's phase concerning the previous example. As with beam production, such beam separation can be accomplished using single or multiple UCAs. In the former situation, a divider is installed between the antenna components and phase shifters.

Many diverse tests have proven the viability of OAMM[94,96,97]. Yan et al. showed 32 Gbps OAMM across a 60 GHz mm-wave band with four concurrent OAM modes (mode=−3, −1, 1 and 3) with 16 QAM modulation. The transmission distance was 2.5 meters, and a 4 to 1 combiner was employed to multiplex 4 SPPs[96]. Mahmouli et al. used a holographic plate and spiral phase plate to transmit 4 Gbps uncompressed video over a 60 GHz mm-wave frequency[97]. Over 10 meters, however, no Gbps level transmission trials have been documented. When a UCA is employed for OAM beam production,

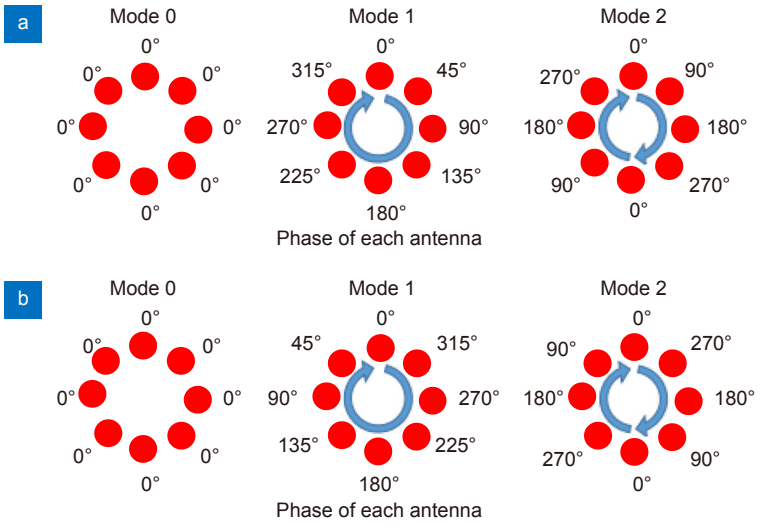

Fig. 12 | (**a**) Formation of OAM modes with a UCA. (**b**) Separation of OAM modes with a UCA.

the capacity upper limit of OAM multiplexing is not superior to that of MIMO technology, according to ref.[98]. Mohammadi et al. investigated the performance of the system as a whole[99]. In ref.[100], the link budget was examined while the mode dependency of the propagation loss was clarified. Significant research has been done and is currently being done, such as studies on calibration techniques[101], examination of the impacts of multipath[102], and so on[103], in addition to the work described above.

A marriage of WDM, MDM and PDM techniques

Different multiplexing techniques such as WDM, PDM, SDM and MDM are presented in previous sections have been established recently. However, it is attractive to cultivate hybrid multiplexing methods to allow enhanced channel numbers. Numerous Si-based on-chip hybrid MUX/DEMUX are demonstrated by integrating more than one multiplexing technique, as shown in Fig. 13. In this section, we will look at the recent development of on-chip hybrid MUX/DEMUX by utilizing hybrid WDM-PDM, WDM-MDM and PDM-MDM techniques.

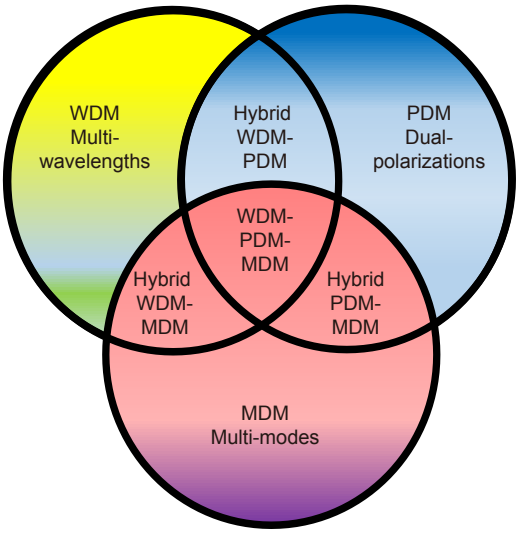

Fig. 13 | Hybrid MUX/DEMUX techniques combing multiple individual methods.

Hybrid WDM-PDM technique

Two attractive techniques such as WDM and the PDM are combined to realize on-chip hybrid WDM-PDM MUX/DEMUX by integrating WDM and polarization manipulating components on the same chip. Array waveguide gratings (AWGs) are widely used in multi-channel WDM networks. Recently, a hybrid WDM-PDM MUX/DEMUX based on the SOI platform is established by incorporating an $(N + 1) \times (N + 1)$ bi-directional AWG with a polarization-diversity circuit (PDC). An 18-channel hybrid WDM-PDM MUX/DEMUX comprising of a 10×10 bi-directional AWG MUX/DEMUX and a PDC was established[104]. The graphical representation of the hybrid MUX/DEMUX is shown in Fig. 14(a). The magnified image of the polarization diversity circuit connecting with the two input WGs of the bi-directional AWG is presented in Fig. 14(b). The PDC consists of a PBS and a polarization rotator (PR). By employing a polarization-selective evanescent coupling in a bent DC, the PBS is apprehended, while the PR is realized in a corner-cut SOI WG by the intervention of two hybridized modes[105]. Both the PBS and PR operate effectively in a wide wavelength range to be well-suited with the WDM network. The CT and the surplus loss of the AWG could be minimized for realistic applications. One might find that the efficiency of the AWG sturdily relies on the spacing of the channel. The dimensions of the AWG circuit increase as the channel spacing reduces, and more phase errors appear, which introduces larger CT. The channel spacing of 3.2, 2, and 0.8 nm leads to the channel CTs of −17 – −23 dB, −15 – −20 dB, and −9 – −15 dB, respectively[106]. To realize efficient SOI-WG AWGs with a slender channel-spacing is still very challenging.

Micro-ring resonators (μ-RRs) have also been extensively used for the realization of low-loss and low-CT WDM filters. The μ-RRs based on SOI WGs are quite compact due to the formation of μ-bends[78,72,107]. Consequently, μ-RRs based on the SOI platform typically have a wide free spectral range (FSR) ~20−30 nm, which is adequate for DWDM networks to span several wavelength channels. Additionally, by optimizing the coupling coefficients, box-like filtering feedback is created by adding an array of μ-rings[108]. A new hybrid PDM-WDM MUX is proposed by incorporating an arrangement of optical filters established on μ-RR and a polarization-splitter-rotator (PSR)[47]. A configuration comprised of an adiabatic taper, an ADC and an MMI mode filter is used for the PSR demonstrating an outstanding efficiency in a wide wavelength range in comparison with a previously reported device[109]. To streamline the circuit arrangement and the wavelength synchronization of the μ-RRs, the cross- and through-ports for all the optical filters based on μ-RR of the PSR are linked via the bus WG. More prominently, these μ-RRs are wavelength selective for TE polarized light and offer

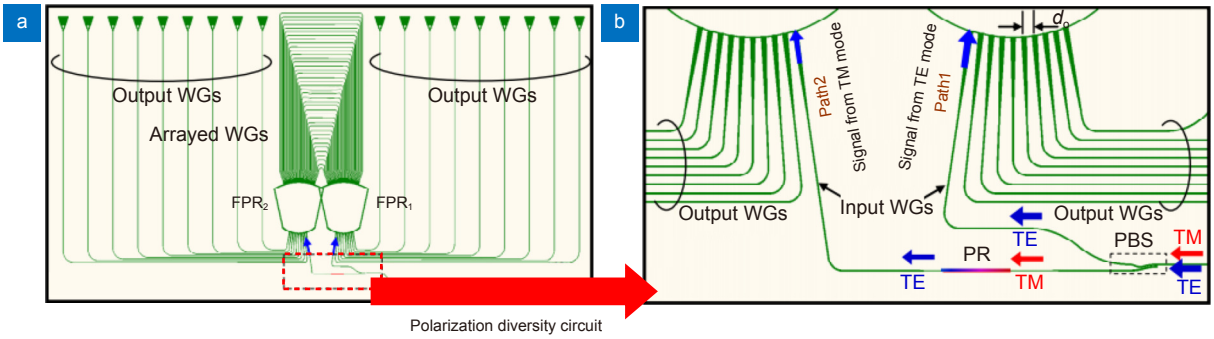

Fig. 14 | (**a**) Graphical pattern of the hybrid MUX/DEMUX containing a bi-directional AWG and a polarization diversity circuit. (**b**) The magnified image of the PDC joining the two input WGs of the bi-directional AWG. Figure reproduced with permission from ref.[104], Optica Publishing Group, under the Optica Open Access Publishing Agreement.

extremely high ER>35 dB which significantly decreases the polarization CT owing to the PSR.

SDM which involves the use of distinct modes in a FMF, is a recognized prospective technique for tackling the high capacity and high bandwidth density demands in future data centers, owning to the exponential development of data traffic in recent years. A mode multiplexer for FMF that is dependable, efficient, and low-cost is thus urgently desired. Integrated diffraction grating produced on the SOI substrate, in addition to fiber-based photonic lanterns and laser inscribed 3D optical WGs, is a possible contender. Low cost, great reliability, mass-production, and co-integration with other integrated photonic devices such as high-bandwidth transceivers are all apparent advantages of monolithic integration[110,111].

Hybrid WDM-MDM technique

One more operational method is to create a hybrid MUX/DEMUX technology that allows WDM and MDM simultaneously to additionally increase the volume of an optical link when N number of wavelengths are accessible. It is conceivable to acquire a high-volume data communication with overall $M \times N$ channels when M modes and N wavelengths are available by utilizing multimode optical WGs capable of supporting multiple guided modes[112,67,14]. Recently, Photonic crystals (PhCs) have been suggested for the realization of PICs due to their outstanding efficiency and small footprint[114,115]. The photonic bandgap (PBG) produced by the periodically modulated refractive index has been employed in various ways to manipulate light[75]. Compared to traditional counterparts, several devices have been introduced using PhCs with promising efficiency and footprint[116–118]. Hybrid WDM/MDM networks have been studied in ref.[119–123].

A WDM/MDM scheme based on the SOI platform has been presented in ref.[124] and the graphical image of the device is displayed in Fig. 15(a). It utilizes strip WGs to realize MMI and DCs for multiplexing. While its performance is acceptable, it has a large footprint. A similar issue has been noted in the devices based on cascaded RRs and DCs[125]. The SEM image of the manufactured hybrid WDM-MDM device is displayed in Fig. 15(b–e). Recently, a novel design of a hybrid WDM-MDM MUX/DEMUX is suggested which is based on a 2D PhC structure[126]. The device is capable of simultaneously multiplexing two modes and two wavelengths. WDM and MDM functions are realized by utilizing two identical MMI couplers and asymmetric DCs, respectively. Tapers are employed at WG intersections to evade back reflections. The device has a small footprint which is appropriate for on-chip incorporation. Numerical calculations disclose that the IL and CT are smaller than 1.0927 dB and −11.9024 dB, respectively, for all four channels. The device configuration is shown in Fig. 15(f).

Hybrid PDM-MDM technique

It is still a difficult task to realize innovative devices that allow extra channels for a single wavelength to attain ultra-high-volume optical interconnects. The channel volume can be improved significantly by adding dual polarization or several guided modes. It is undoubtedly conceivable to mix several guided modes and dual polarizations in such a manner that many channels can be acquired for a single wavelength carrier[18]. Hybrid PDM-MDM MUX/DEMUX is considered as the main component operating with both dual-polarization and multiple modes[128–131]. On-chip PDM and MDM devices based on the Si platform have recently been documented which can provide ultra-compact, CMOS-compatible,

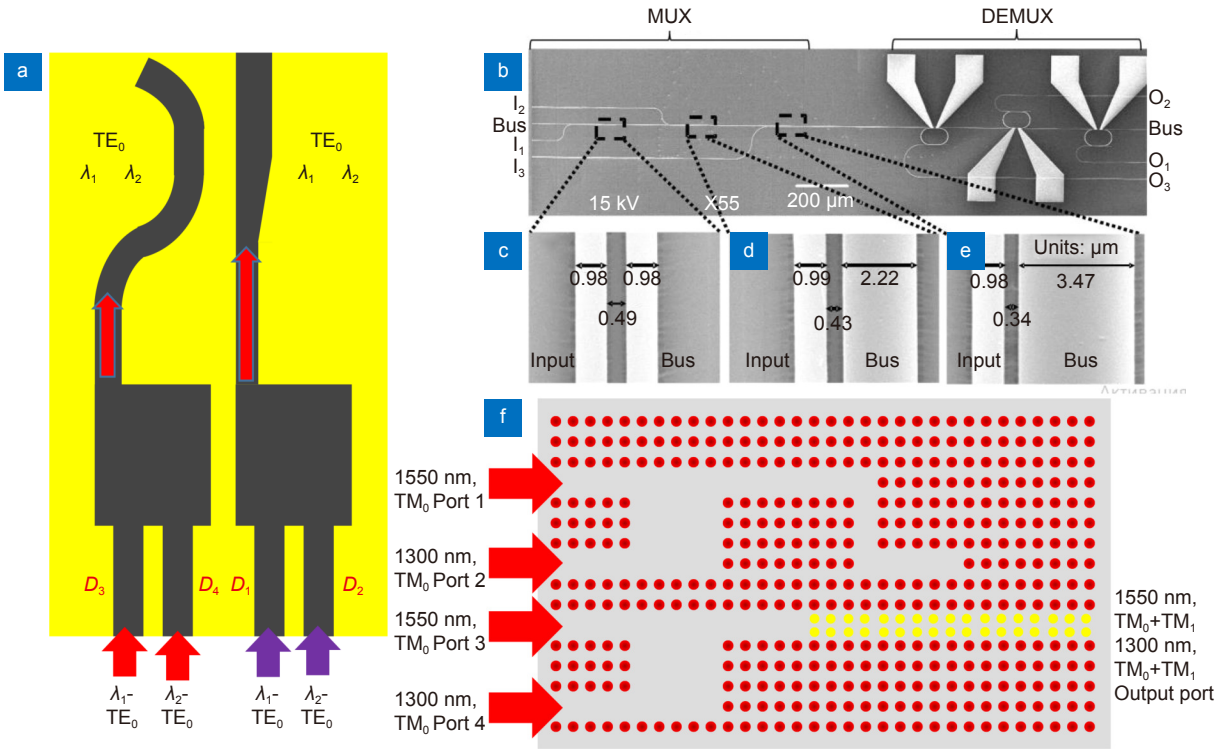

Fig. 15 | (**a**) Schematic representation of a silicon hybrid de (multiplexer) for MDM and WDM. (**b**) SEM image of the manufactured SiN hybrid MDM-WDM device. SEM pictures of the coupling regions between the input WGs and the bus WGs with a designed bus WG width of, (**c**) 1 μm, (**d**) 2.25 μm, (**e**) 3.5 μm. (**f**) Schematic representation of a hybrid WDM-MDM MUX/DEMUX. Figure reproduced from: (a) ref.[124], (b–e)[125], Optica Publishing Group, under the Optica Open Access Publishing Agreement; (f) ref.[126], Optical Society of America.

and low-cost modules[132]. To realize both the polarization and mode MUX/DEMUXs, two methods were proposed, "mode evolution" and "mode coupling"[133,15]. A variety of ACs[134], MMI couplers[135], and Y-branches[136] based architectures have been realized for the polarization or a mode MUX/DEMUX in the view of mode evolution approach. While it is possible to obtain wide BWs and high ERs for these devices, due to the mode evolution method, the footprints are relatively large. Various asymmetric directional couplers (ADCs)[137], grating-assisted ADCs[138], and compactly packed WG arrays (DPWAs)[139] have been shown to achieve ultra-compact polarization and mode MUX/DEMUXs for the mode coupling approach. The advantages of multi-core and multimode techniques are combined in DPWA structure and rather than employing a single broad multimode WG, the DPWA employs a series of thin SOI wire WGs of varying widths. The effective width of the DPWA bus WG is equivalent to that of a standard multimode WG since these WGs are tightly packed with nanometers size gaps. It is possible to develop an efficient and parallel DEMUX technique with a large working wavelength range. However, among these described MUX/DEMUXs, two polarizations with only one fundamental mode were controlled in a polarization MUX/DEMUX or two modes of only single-polarization were maintained in a mode MUX/DEMUX. For the realization of the on-chip hybrid MUX network, a compact, scalable, and broadband MUX/DEMUX supporting more effective modes on dual-polarization is critical.

In ref.[13], a compact Si 10-mode hybrid MUX/DEMUX is demonstrated established on 3-cascaded asymmetric directional couplers (ADCs) based segments, 3-adiabatic tapers, and a PBS. The phase-matching can be attained by changing the widths of the bus WGs and access WGs for the TM modes and TE modes, respectively. The numerical calculations display that a total coupling length for TM_1–TM_3 and TE_1–TE_5 modes can be attained to be 55.4 μm. Besides, the aggregate loss of the hybrid MUX/DEMUX can be minimized due to the fewer tapers in comparison with the standard cascaded ADCs. Likewise, PBS is optimized with a small footprint of 7.0 μm and high extinction ratios of 32.9 dB and 15.4 dB for the TM_0 and TE_0 modes, respectively. The schematic representation of the hybrid MUX/DEMUX is shown in Fig. 16. Moreover, we have listed some most prominent

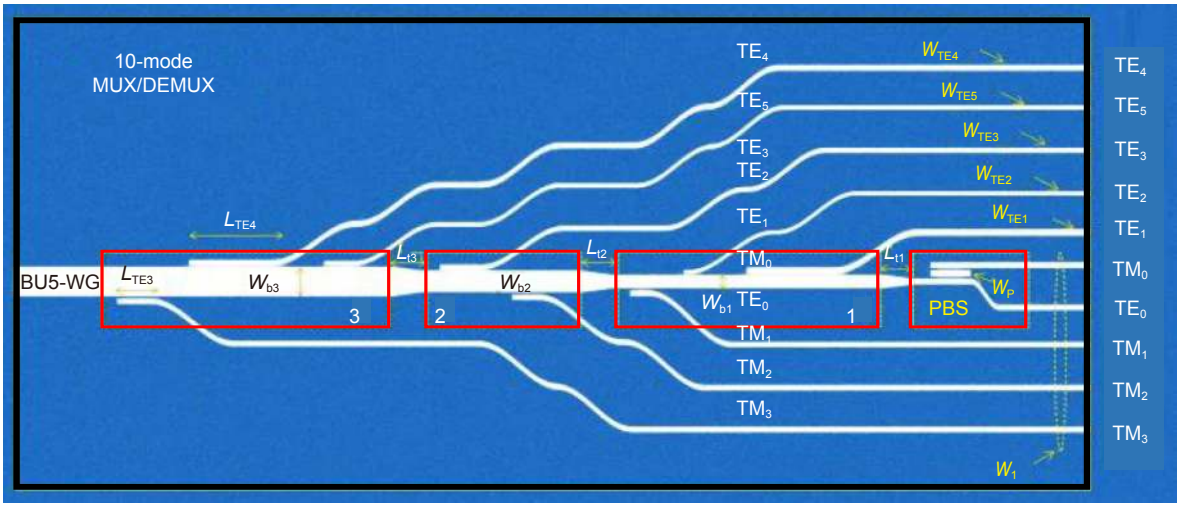

Fig. 16 | Graphical illustration of 10-mode hybrid MUX/DEMUX device for both TE and TM polarizations. Figure reproduced with permission from ref.[13], under a Creative Commons Attribution 4.0 International License.

Table 1 | Few major optical multiplexing papers reported in recent times. IL: Insertion loss, CT: Crosstalk, BW: Bandwidth, MT: Multiplexing technique.

Ref	Year	IL (dB)	CT (dB)	BW (nm)/$\Delta\lambda_{ch}$ (nm)	MT
ref.[140]	2020	<4	–9.5	70	MDM
ref.[141]	2020	0.08, 0.19, 0.03	20	75	MDM
ref.[142]	2020	<0.5	–20	80	MDM
ref.[143]	2020	<1.1	–18	120	MDM
ref.[144]	2013	<1.5	<–9	100	MDM
ref.[145]	2013	~0.3	<–36	100	MDM
ref.[91]	2013	0.3	–16	100	MDM
ref.[146]	2021	1.6	10	90	Hybrid PDM-MDM
ref.[147]	2021	–	–49.93 to –45.8	164–310	WDM
ref.[148]	2018	0.32	–30	90	MDM
ref.[149]	2020	–	–23	260	MDM
ref.[150]	2019	–	–25	140	CWDM
ref.[151]	2014	0.6	–22	35	Hybrid MDM-WDM
ref.[104]	2015	7	–13	3.2	Hybrid WDM-PDM
ref.[152]	2016	1	<-22	3	Hybrid WDM-MDM
ref.[47]	2018	0.5–5.0	–16.5	3.2	Hybrid WDM-MDM

research publications on the multiplexing techniques discussed in this paper as shown in Table 1.

Author's commentary on multiplexing

In this section, we would like to share some of our contributions related to the multiplexing techniques. In our previous work, we have theoretically and experimentally demonstrated the rotation of multimode light beams[153–155], mode division multiplexing[23,156,20], fabrication of diffractive optical elements for optical expansion of laser fields by the orthogonal basis[21,157–162], diffractive optical elements for spatial multiplexing[163–169] and laser ablation and matter structuring[170–173]. Diffractive optics tools such as diffractive optical elements (DOEs) or spatial light modulators (SLMs) can be used both to efficient multiplexing structured laser beams for free-space optical (FSO) information broadcast or input into single- or multi-core fibers, and subsequent DEMUX of the signal at the output of the broadcast network[174]. The most advantageous feature of the FSO is the practically unlimited BW at optical frequencies. However, the effects of the natural random media significantly limit the possibilities of the optical broadcast of information in free space. To overcome this problem, researchers suggest using: partially coherent radiation[175–182]. DOEs are an effective tool not only for generating various types of laser beams

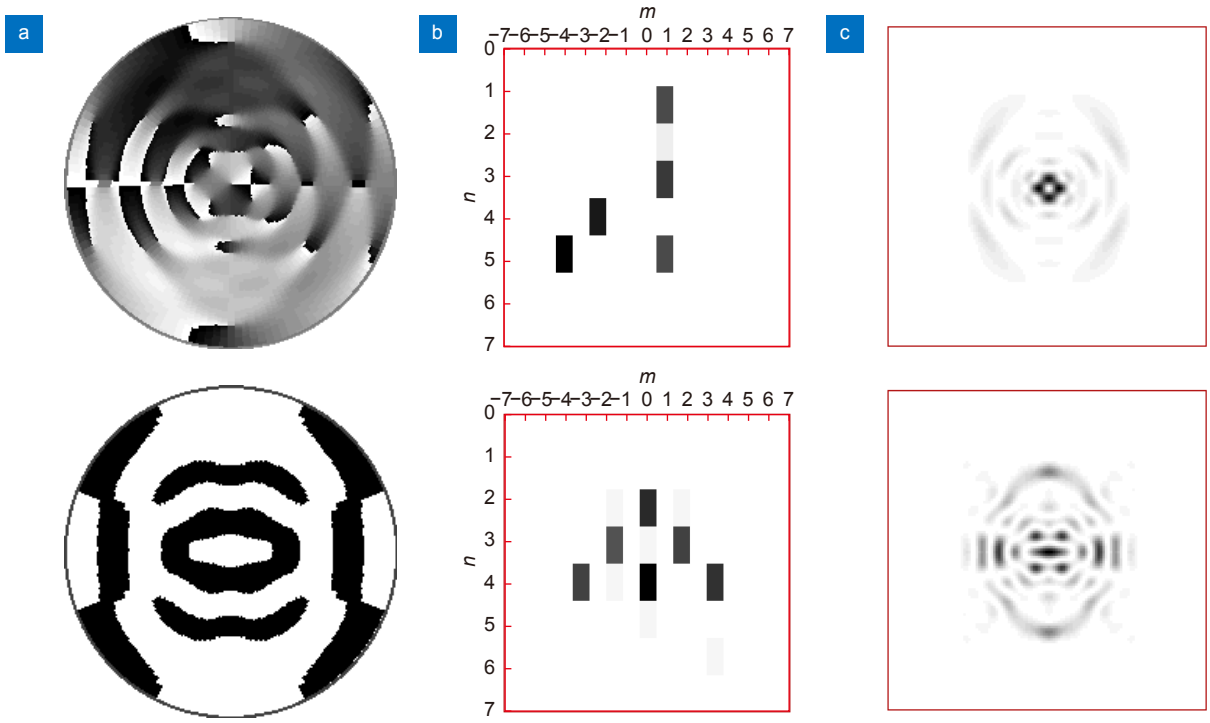

Fig. 17 | Multimode Laguerre-Gauss beams. (**a**) The DOE phase. (**b**) The squared modulus of the coefficients in the superposition. (**c**) The intensity distributions in the focal plane for 5-modes beam (the upper row) and the 6-modes beam (the bottom row). Figure reproduced from ref.[154], American Institute of Physics.

but also for their superposition with desired properties which can be used for MDM resistance to FSO turbulence influence[183,153–155]. Figure 17 illustrates phase DOEs for efficient generation multimode Laguerre-Gauss beams with 5 desired modes of indices (n, m)=(1, 1)+(3, 1)+(4, −3)+(5, −5)+(5, 1) (the upper row, 16-level phase) and with 6 desired modes of indices (n,m)=(2, 0)+(3, −2)+(3, 2)+(4, −4)+(4, 0)+(4, 4) (the bottom row, binary phase).

Also, utilizing diffractive optics any pattern of modes with preferred weights can be effectively excited in FOs[184–188]. Figure 18 shows simulation results of excitation and propagation of selected LP modes in a weakly guiding step-index FO.

DOEs that produce a variety of mode beams in different diffraction orders[157–161] are used as spatial filters to investigate the transverse mode characteristic of light and achieve DEMUX at the output of the optical transmitting information network[189–192]. Figure 19 shows the correlation network with a multi-channel DOE for

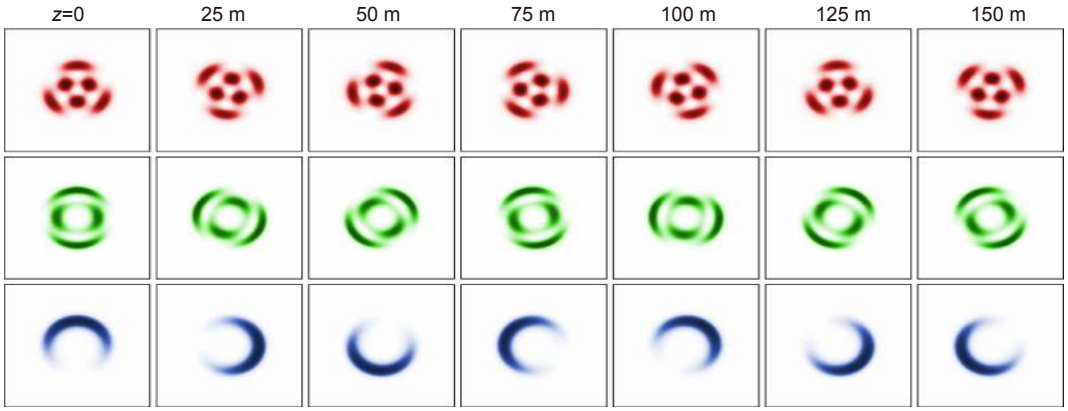

Fig. 18 | Propagation of LP modes superposition in a weakly guiding stepped-index FO (the intensity distribution is taken at different distances z) for (p, q)=(1, 2)+(−2, 1) (top row), (p, q)=(3, 2)+(5, 1) (middle row), (p, q)=(4, 1)+(5, 1) (bottom row). Figure reproduced from ref.[189], Pleiades Publishing.

instantaneous recognition of individual vortex positions of different Laguerre-Gaussian beams arbitrary to offset from the optical axis.

Note that in this case, not only MDM is possible, but also the detection of a variety of polarization positions (MDM+PDM)[193–198]. Figure 20 shows binary multi-channel DOE for examining the polarization and phase positions of vortex cylindrically polarized beams.

There are known works where MDM, PDM and WDM are combined[199]. Multi-order optical elements matched with the laser modes[157,159,14,160,21] and DOEs for 1D, 2D and 3D spatial multiplexing of different light

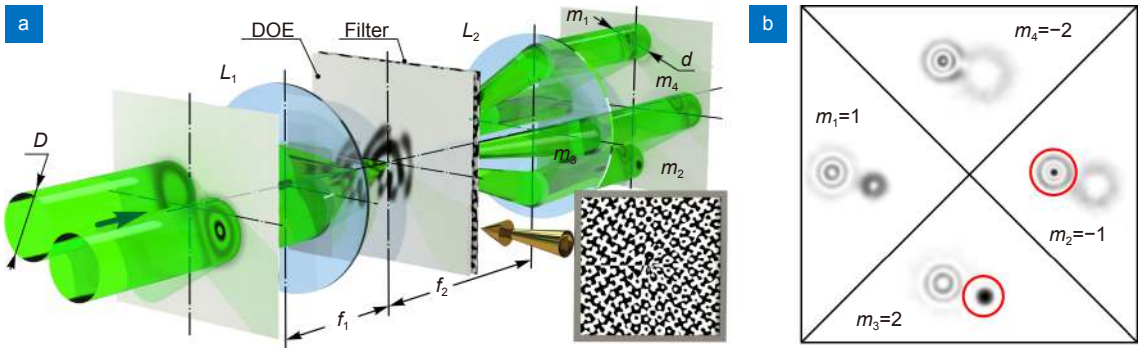

Fig. 19 | Instantaneous recognition of particular vortex positions of Laguerre–Gaussian beams. (**a**) The correlation network with a multi-channel DOE. (**b**) Results of detection (correlation peaks circled in red) in the focal plane. Figure reproduced from ref.[192], under a Creative Commons Attribution.

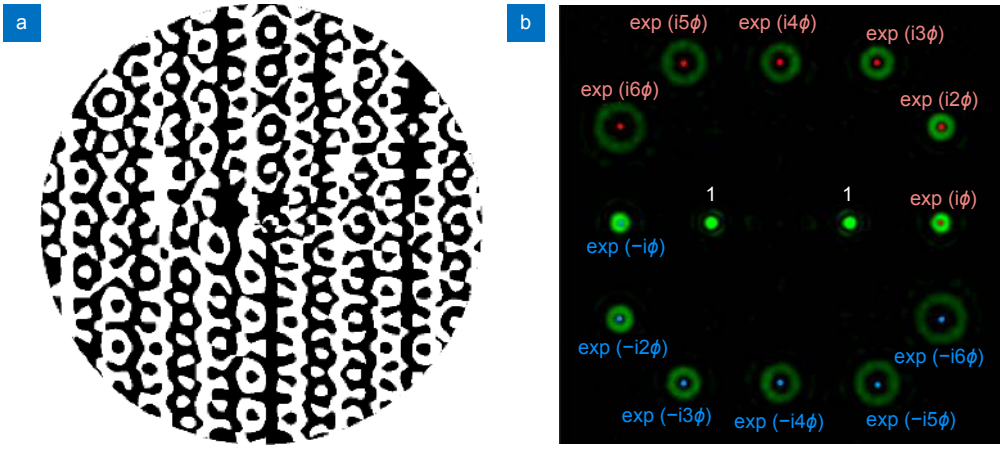

Fig. 20 | Binary 14-channel DOE for investigating the polarization and phase positions of vortex cylindrically polarized beams. (**a**) DOE phase. (**b**) Correspondence of the diffraction orders in the focal plane to the orders of optical vortices[198].

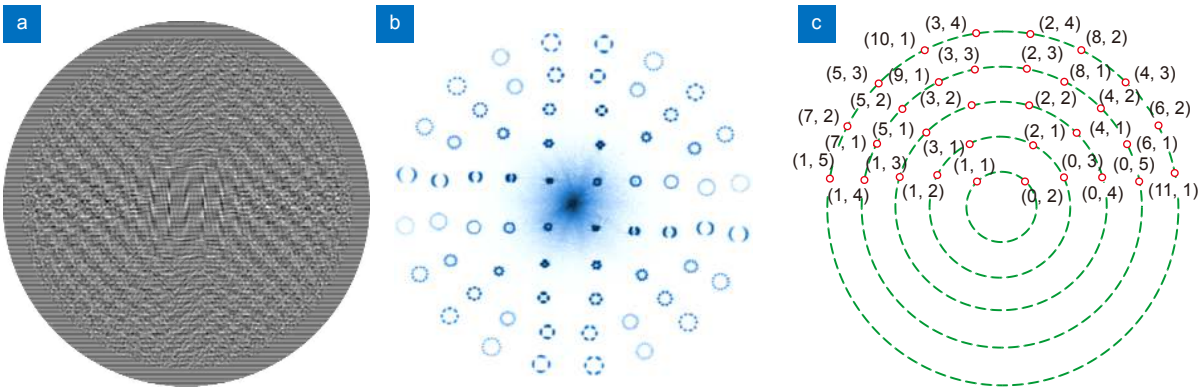

Fig. 21 | (**a**) The binary phase of the encoded 64-order DOE, matched with LP modes of a step-index FO. (**b**) The experimentally recorded intensity distribution in the focal plane of the lens when the DOE is illuminated by a plane wave. (**c**) The arrangement of LP-modes indices $p = \overline{0,11}$, $q = \overline{1,5}$ (the conjugate modes with indices $p = \overline{-11,0}$ are located symmetrically in the lower part). Figure reproduced with permission from ref.[156], under a Creative Commons Attribution 4.0 International License.

elements/units/primitives (light spots, rings, lines, etc.)[165,167,163,164,169,170] can be used to generate beams arrays for SDM[200,201] and perform the simultaneous coupling of light into a set of FOs, including MIMO[202,203,156,67,204,205]. Figure 21 illustrates multi-channel binary phase DOE matched with LP modes of a step-index FO which can be used to detect 64 modes simultaneously. The results and discussion should be presented in a logical sequence in the text, tables, and figures; repetitive presentation of the same data in different forms should be avoided. This section should consider the experimental results concerning any hypotheses advanced in the Introduction.

Concluding remarks

In conclusion, we have presented a detailed review of the recent advances in multiplexing techniques that can be utilized in fiber optics and on-chip communication. Optical multiplexing is the practice of merging several optical signals into one to make maximum use of the gigantic bandwidth volume of an optical channel. The concept is to split the vast bandwidth of fiber optics into individual low bandwidth channels so that multiple access is accomplished through lower-speed electronics. The historic background of the multiplexing can be found in the Introduction section. The recent developments in the field of WDM, PDM, SDM, MDM and OAMM can be found in the successive sections. Moreover, three different kinds of on-chip hybrid MUX/DEMUXs are considered which are formed by the integration of WDM with PDM, MDM with WDM and MDM with PDM techniques as shown in Fig. 13. Hybrid MUX/DEMUXs are formed as the result of the marriage of various WDM, PDM and MDM elements such as arrayed waveguide gratings (AWGs), micro-ring resonators (μ-RRs), polarization-splitter-rotators (PSRs) and couplers. Two common WDM strategies exist, i.e., AWGs and μ-RRs, which are effectively comprehended when wide channel spacing is adequate. Yet, it is not possible to accomplish lossless and low-CT AWGs or μ-RRs having compact channel spacing. Auspiciously, by optimizing the design and the manufacturing methods, this can be solved. In recent times, high performance PDM devices comprise polarization rotators (PRs), and PSRs are industrialized. As a new functional component, different structures have been used to develop MDM devices. For any hybrid MUX/DEMUX networks realized with the MDM method, low-loss and low-CT multimode operation is considerably preferred. By exploiting these vital devices, numerous on-chip hybrid MUX/DEMUX has been apprehended which results in a significant increase in the channel number to augment the link volume of optical interconnects.

References

1. Gnauck AH, Tkach RW, Chraplyvy AR, Li T. High-capacity optical transmission systems. *J Lightwave Technol* **26**, 1032–1045 (2008).
2. Rademacher G, Luís RS, Puttnam BJ, Eriksson TA, Agrell E et al. 159 Tbit/s C+L band transmission over 1045 km 3-mode graded-index few-mode fiber. In *Proceedings of the Optical Fiber Communication Conference 2018* 1–3 (Optica Publishing Group, 2018); http://doi.org/10.1364/OFC.2018.Th4C.4.
3. Saliba SD, Scholten RE. Linewidths below 100 kHz with external cavity diode lasers. *Appl Opt* **48**, 6961–6966 (2009).
4. Keaveney J, Hamlyn JW, Adams CS, Hughes IG. A single-mode external cavity diode laser using an intra-cavity atomic Faraday filter with short-term linewidth <400 kHz and long-term stability of < 1 MHz. *Rev Sci Instrum* **87**, 095111 (2016).
5. Baeuerle B, Heni W, Hoessbacher C, Fedoryshyn Y, Koch U et al. 120 GBd plasmonic Mach-Zehnder modulator with a novel differential electrode design operated at a peak-to-peak drive voltage of 178 mV. *Opt Express* **27**, 16823–16832 (2019).
6. Hiraki T, Aihara T, Takeda K, Fujii T, Kakitsuka T et al. Membrane InGaAsP Mach-Zehnder modulator with SiN: D waveguides on Si platform. *Opt Express* **27**, 18612–18619 (2019).
7. Ahmed M. Effect of fiber attenuation and dispersion on the transmission distance of 40-Gb/s optical fiber communication systems using high-speed lasers. *Phys Wave Phen* **22**, 266–272 (2014).
8. Kani J, Iwatsuki K, Imai T. Optical multiplexing technologies for access-area applications. *IEEE J Sel Top Quantum Electron* **12**, 661–668 (2006).
9. Bergano NS, Davidson CR. Wavelength division multiplexing in long-haul transmission systems. *J. Lightwave Technol* **14**, 1299–1308 (1996).
10. Chen ZY, Yan LS, Pan Y, Jiang L, Yi AL et al. Use of polarization freedom beyond polarization-division multiplexing to support high-speed and spectral-efficient data transmission. *Light Sci Appl* **6**, e16207 (2017).
11. Fazea Y, Mezhuyev V. Selective mode excitation techniques for mode-division multiplexing: a critical review. *Opt Fiber Technol* **45**, 280–288 (2018).
12. Wang SP, Wu H, Zhang M, Dai DX. A 32-channel hybrid wavelength-/mode-division (de) Multiplexer on silicon. *IEEE Photonics Technol Lett* **30**, 1194–1197 (2018).
13. Jiang WF, Miao JY, Li T. Compact silicon 10-mode multi/demultiplexer for hybrid mode- and polarisation-division multiplexing system. *Sci Rep* **9**, 13223 (2019).
14. Pan TH, Tseng SY. Short and robust silicon mode (de)multiplexers using shortcuts to adiabaticity. *Opt Express* **23**, 10405–10412 (2015).
15. Jiang WF. Ultra-compact and fabrication-tolerant mode multiplexer and demultiplexer based on angled silicon waveguides. *Opt Commun* **425**, 141–145 (2018).
16. Li HQ, Wang PJ, Yang TJ, Dai TG, Wang GC et al. Experimental demonstration of a broadband two-mode multi/demultiplexer based on asymmetric Y-junctions. *Opt Laser Technol* **100**, 7–11 (2018).

17. Uematsu T, Ishizaka Y, Kawaguchi Y, Saitoh K, Koshiba M. Design of a compact two-mode multi/demultiplexer consisting of multimode interference waveguides and a wavelength-insensitive phase shifter for mode-division multiplexing transmission. *J Lightwave Technol* **30**, 2421–2426 (2012).
18. Dai DX, Wang SP. Asymmetric directional couplers based on silicon nanophotonic waveguides and applications. *Front Optoelectron* **9**, 450–465 (2016).
19. Li HQ, Li SQ, Yang TJ, Xu JY, Li J et al. Silicon two-mode multi/demultiplexer based on tapered couplers. *Optik* **176**, 518–522 (2019).
20. Kazanskiy NL, Khonina SN, Karpeev SV, Porfirev AP. Diffractive optical elements for multiplexing structured laser beams. *Quantum Electron* **50**, 629–635 (2020).
21. Porfirev AP, Fomchenkov SA, Gridin GE, Khonina SN. Binary diffractive optics for 3D-demultiplexing of OAM beams. *J Phys:Conf Ser* **1124**, 051015 (2018).
22. Khonina SN, Kazanskiy NL, Soifer VA. Optical vortices in a fiber: mode division multiplexing and multimode self-imaging. In Yasin M, Harun SW, Arof H. *Recent Progress in Optical Fiber Research*. IntechOpen Publisher, Croatia, 2012.
23. Karpeev SV, Pavelyev VS, Soifer VA, Khonina SN, Duparre M et al. Transverse mode multiplexing by diffractive optical elements. *Proc SPIE* **5854**, 1–12 (2005).
24. Stark JB, Mitra P, Sengupta A. Information capacity of nonlinear wavelength division multiplexing fiber optic transmission line. *Opt Fiber Technol* **7**, 275–288 (2001).
25. Secondini M, Forestieri E. The limits of the nonlinear Shannon limit. In *Proceedings of 2016 Optical Fiber Communications Conference and Exhibition* (IEEE, 2016). https://doi.org/10.1 364/OFC.2016.Th3D.1
26. Armstrong J. OFDM for optical communications. *J Lightwave Technol* **27**, 189–204 (2009).
27. Chow CW, Yeh CH, Wang CH, Wu CL, Chi S et al. Studies of OFDM signal for broadband optical access networks. *IEEE J Sel Area Commun* **28**, 800–807 (2010).
28. Gunawan WH, Liu Y, Chow CW, Chang YH, Yeh CH. High speed visible light communication using digital power domain multiplexing of orthogonal frequency division multiplexed (OFDM) signals. *Photonics* **8**, 500 (2021).
29. Saito Y, Kishiyama Y, Benjebbour A, Nakamura T, Li AX et al. Non-orthogonal multiple access (NOMA) for cellular future radio access. In *Proceedings of the 77th Vehicular Technology Conference* (*VTC Spring*) 1–5 (IEEE, 2013); http://doi.org/10.1109/VTCSpring.2013.6692652.
30. DeLange OE. Wide-band optical communication systems: part II-Frequency-division multiplexing. *Proc IEEE* **58**, 1683–1690 (1970).
31. Nosu K, Ishio H. A design of optical multi/demultiplexers for optical wavelength-division multiplexing transmission. *Trans IECE* **62-B**, 1030–1036 (1979).
32. Tomlinson WJ. Wavelength multiplexing in multimode optical fibers. *Appl Opt* **16**, 2180–2194 (1977).
33. Senior JM, Cusworth SD. Wavelength division multiplexing in optical fibre sensor systems and networks: a review. *Opt Laser Technol* **22**, 113–126 (1990).
34. Ishio H, Minowa J, Nosu K. Review and status of wavelength-division-multiplexing technology and its application. *J Lightwave Technol* **2**, 448–463 (1984).
35. Li CY, Lu HH, Tsai WS, Feng CY, Chou CR et al. White-light-ing and WDM-VLC system using transmission gratings and an engineered diffuser. *Opt Lett* **45**, 6206–6209 (2020).
36. Liu Z, Zhang JS, Li XL, Wang LL, Li JG et al. 25×50 Gbps wavelength division multiplexing silicon photonics receiver chip based on a silicon nanowire-arrayed waveguide grating. *Photonics Res* **7**, 659–663 (2019).
37. Richardson DJ, Fini JM, Nelson LE. Space-division multiplexing in optical fibres. *Nat Photonics* **7**, 354–362 (2013).
38. Goossens JW, Yousefi MI, Jaouën Y, Hafermann H. Polarization-division multiplexing based on the nonlinear Fourier transform. *Opt Express* **25**, 26437–26452 (2017).
39. Hayee MI, Cardakli MC, Sahin AB, Willner AE. Doubling of bandwidth utilization using two orthogonal polarizations and power unbalancing in a polarization-division-multiplexing scheme. *IEEE Photonics Technol Lett* **13**, 881–883 (2001).
40. Hill PM, Olshansky R, Burns WK. Optical polarization division multiplexing at 4Gb/s. *IEEE Photonics Technol Lett* **4**, 500–502 (1992).
41. Evangelides SG, Mollenauer LF, Gordon JP, Bergano NS. Polarization multiplexing with solitons. *J Lightwave Technol* **10**, 28–35 (1992).
42. Han Y, Li G. Experimental demonstration of direct-detection quaternary differential polarisation-phase-shift keying with electrical multilevel decision. *Electron Lett* **42**, 109–111 (2006).
43. Noe R, Hinz S, Sandel D, Wust F. Crosstalk detection schemes for polarization division multiplex transmission. *J Lightwave Technol* **19**, 1469–1475 (2001).
44. Coura DJC, Silva JAL, Segatto MEV. A bandwidth scalable OFDM passive optical network for future access network. *Photon Netw Commun* **18**, 409 (2009).
45. Morant M, Llorente R, Hauden J, Quinlan T, Mottet A et al. Dual-drive $LiNbO_3$ interferometric Mach-Zehnder architecture with extended linear regime for high peak-to-average OFDM-based communication systems. *Opt Express* **19**, B452–B458 (2011).
46. Qiu HY, Yu H, Hu T, Jiang GM, Shao HF et al. Silicon mode multi/demultiplexer based on multimode grating-assisted couplers. *Opt Express* **21**, 17904–17911 (2013).
47. Tan Y, Wu H, Wang SP, Li CL, Dai DX. Silicon-based hybrid demultiplexer for wavelength-and mode-division multiplexing. *Opt Lett* **43**, 1962–1965 (2018).
48. Sun CL, Yu Y, Chen GY, Zhang XL. Integrated switchable mode exchange for reconfigurable mode-multiplexing optical networks. *Opt Lett* **41**, 3257–3260 (2016).
49. Guan XW, Ding YH, Frandsen LH. Ultra-compact broadband higher order-mode pass filter fabricated in a silicon waveguide for multimode photonics. *Opt Lett* **40**, 3893–3896 (2015).
50. Han LS, Kuo BPP, Alic N, Radic S. Ultra-broadband multimode 3dB optical power splitter using an adiabatic coupler and a Y-branch. *Opt Express* **26**, 14800–14809 (2018).
51. Zhang Y, He Y, Zhu QM, Qiu CY, Su YK. On-chip silicon photonic 2×2 mode-and polarization-selective switch with low inter-modal crosstalk. *Photonics Res* **5**, 521–526 (2017).
52. Khan LU. Visible light communication: applications, architecture, standardization and research challenges. *Digit Commun Netw* **3**, 78–88 (2017).
53. Vega-Colado C, Arredondo B, Torres JC, López-Fraguas E, Vergaz R et al. An all-organic flexible visible light communication system. *Sensors* **18**, 3045 (2018).
54. Wang YQ, Yang C, Wang YG, Chi N. Gigabit polarization

division multiplexing in visible light communication. *Opt Lett* **39**, 1823–1826 (2014).
55. Perkins R, Gruev V. Signal-to-noise analysis of Stokes parameters in division of focal plane polarimeters. *Opt Express* **18**, 25815–25824 (2010).
56. Thangaraj C, Pownall R, Nikkel P, Yuan GW, Lear KL et al. Fully CMOS-compatible on-chip optical clock distribution and recovery. *IEEE Trans Very Scale Integr (VLSI) Syst* **18**, 1385–1398 (2010).
57. Ivanovich D, Powell SB, Gruev V, Chamberlain RD. Polarization division multiplexing for optical data communications. *Proc SPIE* **10538**, 105381D (2018).
58. Kanada T, Franzen DL. Single-mode fiber dispersion measurements using optical sampling with a mode-locked laser diode. *Opt Lett* **11**, 330–332 (1986).
59. Saitoh K, Koshiba M, Takenaga K, Matsuo S. Crosstalk and core density in uncoupled multicore fibers. *IEEE Photonics Technol Lett* **24**, 1898–1901 (2012).
60. Macho A, Morant M, Llorente R. Experimental evaluation of nonlinear crosstalk in multi-core fiber. *Opt Express* **23**, 18712–18720 (2015).
61. Hayashi T, Taru T, Shimakawa O, Sasaki T, Sasaoka E. Design and fabrication of ultra-low crosstalk and low-loss multi-core fiber. *Opt Express* **19**, 16576–16592 (2011).
62. Sasaki Y, Takenaga K, Aikawa K, Miyamoto Y, Morioka T. Single-mode 37-core fiber with a cladding diameter of 248 μm. In *Proceedings of 2017 Optical Fiber Communications Conference and Exhibition* 1–3 (IEEE, 2017). https://doi.org/10.1364/OFC.2017.Th1H.2
63. Abedin KS, Taunay TF, Fishteyn M, DiGiovanni DJ, Supradeepa VR et al. Cladding-pumped erbium-doped multicore fiber amplifier. *Opt Express* **20**, 20191–20200 (2012).
64. Rademacher G, Luís RS, Puttnam BJ, Ryf R, Furukawa H et al. 93.34 Tbit/s/mode (280 Tbit/s) transmission in a 3-mode graded-index few-mode fiber. In *Proceedings of 2018 Optical Fiber Communications Conference and Exposition* 1–3 (IEEE, 2018). https://doi.org/10.1364/OFC.2018.W4C.3
65. Rademacher G, Puttnam BJ, Luís RS, Eriksson TA, Fontaine NK et al. Peta-bit-per-second optical communications system using a standard cladding diameter 15-mode fiber. *Nat Commun* **12**, 4238 (2021).
66. Hayashi T, Tamura Y, Hasegawa T, Taru T. Record-low spatial mode dispersion and ultra-low loss coupled multi-core fiber for ultra-long-haul transmission. *J Lightwave Technol* **35**, 450–457 (2017).
67. van Uden RGH, Correa RA, Lopez EA, Huijskens FM, Xia C et al. Ultra-high-density spatial division multiplexing with a few-mode multicore fibre. *Nat Photonics* **8**, 865–870 (2014).
68. Shibahara K, Lee D, Kobayashi T, Mizuno T, Takara H et al. Dense SDM (12-Core × 3-Mode) transmission over 527 km With 33.2-ns mode-dispersion employing low-complexity parallel MIMO frequency-domain equalization. *J Lightwave Technol* **34**, 196–204 (2016).
69. Puttnam BJ, Rademacher G, Luís RS. Space-division multiplexing for optical fiber communications. *Optica* **8**, 1186–1203 (2021).
70. Jiang WF, Hu JZ, Mao SQ, Zhang HY, Zhou LJ et al. Broadband silicon four-mode (de) multiplexer using subwavelength grating-assisted triple-waveguide couplers. *J Lightwave Technol* **39**, 5042–5047 (2021).
71. He Y, Zhang Y, Zhu QM, An SH, Cao RY et al. Silicon high-order mode (de) multiplexer on single polarization. *J Lightwave Technol* **36**, 5746–5753 (2018).
72. Butt MA, Khonina SN, Kazanskiy NL. Highly sensitive refractive index sensor based on hybrid plasmonic waveguide microring resonator. *Waves Random Complex Media* **30**, 292–299 (2020).
73. Butt MA, Khonina SN, Kazanskiy NL. Sensitivity enhancement of silicon strip waveguide ring resonator by incorporating a thin metal film. *IEEE Sens J* **20**, 1355–1362 (2020).
74. Butt MA, Kazanskiy NL. Mode sensitivity analysis of vertically arranged double hybrid plasmonic waveguide. *Opt Adv Mater Rapid Commun* **14**, 385–388 (2020).
75. Kazanskiy NL, Butt MA. One-dimensional photonic crystal waveguide based on SOI platform for transverse magnetic polarization-maintaining devices. *Photonics Lett Poland* **12**, 85–87 (2020).
76. Butt MA, Khonina SN, Kazanskiy NL. Ultrashort inverted tapered silicon ridge-to-slot waveguide coupler at 1.55 μm and 3.392 μm wavelength. *Appl Opt* **59**, 7821–7828 (2020).
77. Khonina SN, Kazanskiy NL, Butt MA. Evanescent field ratio enhancement of a modified ridge waveguide structure for methane gas sensing application. *IEEE Sens J* **20**, 8469–8476 (2020).
78. Butt MA, Khonina SN, Kazanskiy NL. A highly sensitive design of subwavelength grating double-slot waveguide microring resonator. *Laser Phys Lett* **17**, 076201 (2020).
79. Kazanskiy NL, Khonina SN, Butt MA. Subwavelength grating double slot waveguide racetrack ring resonator for refractive index sensing application. *Sensors* **20**, 3416 (2020).
80. Yu F, Yamamoto K, Piao XQ, Yokoyama S. Multimode interference waveguide switch of electro-optic polymer with tapered access waveguides. *Phys Procedia* **14**, 25–28 (2011).
81. Wu XR, Huang CR, Xu K, Shu C, Tsang HK. Mode-division multiplexing for silicon photonic network-on-chip. *J Lightwave Technol* **35**, 3223–3228 (2017).
82. Luo LW, Gabrielli LH, Lipson M. On-chip mode-division multiplexer. In *Proceedings of the CLEO*: *Science and Innovations 2013* 1–2 (Optica Publishing Group, 2013); http://doi.org/10.1364/CLEO_SI.2013.CTh1C.6.
83. Liu YJ, Xu K, Wang S, Shen WH, Xie HC et al. Arbitrarily routed mode-division multiplexed photonic circuits for dense integration. *Nat Commun* **10**, 3263 (2019).
84. He Y, An SH, Li XF, Huang YT, Zhang Y et al. Record high-order mode-division-multiplexed transmission on chip using gradient-duty-cycle subwavelength gratings. In *Proceedings of 2021 Optical Fiber Communications Conference and Exhibition* 1–3 (IEEE, 2021). https://ieeexplore.ieee.org/document/9489861
85. Su YK, He Y, Chen HS, Li XY, Li GF. Perspective on mode-division multiplexing. *Appl Phys Lett* **118**, 200502 (2021).
86. Ding YH, Ou HY, Xu J, Peucheret C. Silicon photonic integrated circuit mode multiplexer. *IEEE Photonics Technol Lett* **25**, 648–651 (2013).
87. Koonen AMJ, Chen HS, van den Boom HPA, Raz O. Silicon photonic integrated mode multiplexer and demultiplexer. *IEEE Photonics Technol Lett* **24**, 1961–1964 (2012). 88. https://doi.org/10.1109/LPT.2012.2219304
88. Li CL, Liu DJ, Dai DX. Multimode silicon photonics. *Nanophotonics* **8**, 227–247 (2018).

89. Dai DX. Silicon mode-(de) multiplexer for a hybrid multiplexing system to achieve ultrahigh capacity photonic networks-on-chip with a single-wavelength-carrier light. In *Proceedings of 2012 Asia Communications and Photonics Conference* 1–3 (IEEE, 2012). https://ieeexplore.ieee.org/abstract/document/6510982
90. Binici HI. Controlling light inside a multi-mode fiber by wavefront shaping. (The Graduate School of Natural and Applied Sciences of Middle East Technical University, 2018). http://dx.doi.org/10.13140/RG.2.2.35259.52005
91. Ding YH, Xu J, Da Ros F, Huang B, Ou HY et al. On-chip two-mode division multiplexing using tapered directional coupler-based mode multiplexer and demultiplexer. *Opt Express* **21**, 10376–10382 (2013).
92. Dai DX, Wang J, Shi YC. Silicon mode (de)multiplexer enabling high capacity photonic networks-on-chip with a single-wavelength-carrier light. *Opt Lett* **38**, 1422–1424 (2013).
93. Ye MY, Yu Y, Sun CL, Zhang XL. On-chip data exchange for mode division multiplexed signals. *Opt Express* **24**, 528–535 (2016).
94. Yan Y, Xie GD, Lavery MPJ, Huang H, Ahmed N et al. High-capacity millimetre-wave communications with orbital angular momentum multiplexing. *Nat Commun* **5**, 4876 (2014).
95. Lee D, Sasaki H, Fukumoto H, Hiraga K, Nakagawa T. Orbital angular momentum (OAM) multiplexing: an enabler of a new era of wireless communications. *IEICE Trans Commun* **E100-B**, 1044–1063 (2017).
96. Yan Y, Li L, Zhao Z, Xie GD, Wang Z et al. 32-Gbit/s 60-GHz millimeter-wave wireless communication using orbital angular momentum and polarization multiplexing. In *Proceedings of 2016 IEEE International Conference on Communications* (*ICC*) 1–6 (IEEE, 2016); http://doi.org/10.1109/ICC.2016.7511277.
97. Mahmouli FE, Walker SD. 4-Gbps uncompressed video transmission over a 60-GHz orbital angular momentum wireless channel. *IEEE Wireless Commun Lett* **2**, 223–226 (2013).
98. Zhang ZF, Zheng SL, Chen YL, Jin XF, Chi H et al. The capacity gain of orbital angular momentum based multiple-input-multiple-output system. *Sci Rep* **6**, 25418 (2016).
99. Mohammadi SM, Daldorff LKS, Bergman JES, Karlsson RL, Thide B et al. Orbital angular momentum in radio-A system study. *IEEE Trans Antennas Propag* **58**, 565–572 (2010).
100. Cagliero A, De Vita A, Gaffoglio R, Sacco B. A new approach to the link budget concept for an OAM communication link. *IEEE Antennas Wireless Propag Lett* **15**, 568–571 (2015).
101. Tian H, Liu ZQ, Xi W, Nie GF, Liu L et al. Beam axis detection and alignment for uniform circular array-based orbital angular momentum wireless communication. *IET Commun* **10**, 44–49 (2016).
102. Yan Y, Li L, Xie GD, Bao CJ, Liao PC et al. Experimental measurements of multipath-induced intra- and inter-channel crosstalk effects in a millimeter-wave communications link using orbital-angular-momentum multiplexing. In *Proceedings of 2015 IEEE International Conference on Communications* (*ICC*) 1370–1375 (IEEE, 2015); http://doi.org/10.1109/ICC.2015.7248514.
103. Zheng SL, Hui XN, Jin XF, Chi H, Zhang XM. Transmission characteristics of a twisted radio wave based on circular traveling-wave antenna. *IEEE Trans Antennas Wireless Propag Lett* **63**, 1530–1536 (2015).
104. Chen ST, Shi YC, He SL, Dai DX. Compact monolithically-integrated hybrid (de)multiplexer based on silicon-on-insulator nanowires for PDM-WDM systems. *Opt Express* **23**, 12840–12849 (2015).
105. Aamer M, Gutierrez AM, Brimont A, Vermeulen D, Roelkens G et al. CMOS compatible silicon-on-insulator polarization rotator based on symmetry breaking of the waveguide cross section. *IEEE Photonics Technol Lett* **24**, 2031–2034 (2012).
106. Pathak S, Vanslembrouck M, Dumon P, Van Thourhout D, Verheyen P et al. Effect of mask discretization on performance of silicon arrayed waveguide gratings. *IEEE Photonics Technol Lett* **26**, 718–721 (2014).
107. Butt MA, Khonina SN, Kazanskiy NL. Device performance of standard strip, slot and hybrid plasmonic μ-ring resonator: a comparative study. *Waves Random Complex Media* **31**, 2397–2406 (2021).
108. Tan Y, Chen ST, Dai DX. Polarization-selective microring resonators. *Opt Express* **25**, 4106–4119 (2017).
109. Dai DX, Wu H. Realization of a compact polarization splitter-rotator on silicon. *Opt Lett* **41**, 2346–2349 (2016).
110. Tong YY, Zhou W, Wu XR, Tsang HK. Efficient mode multiplexer for few-mode fibers using integrated silicon-on-insulator waveguide grating coupler. *IEEE J Quantum Electron* **56**, 8400107 (2020).
111. Kuo PC, Tong YY, Chow CW, Tsai JF, Liu Y et al. 4.36 Tbit/s silicon chip-to-chip transmission via few-mode fiber (FMF) using 2D sub-wavelength grating couplers. In *Proceedings of the Optical Fiber Communication Conference 2021* (Optica Publishing Group, 2021); http://doi.org/10.1364/OFC.2021.M3D.6.
112. Zhao NB, Li XY, Li GF, Kahn JM. Capacity limits of spatially multiplexed free-space communication. *Nat Photonics* **9**, 822–826 (2015).
113. Rahmani B, Loterie D, Konstantinou G, Psaltis D, Moser C. Multimode optical fiber transmission with a deep learning network. *Light Sci Appl* **7**, 69 (2018).
114. Sharkawy A, Shi SY, Prather DW. Multichannel wavelength division multiplexing with photonic crystals. *Appl Opt* **40**, 2247–2252 (2001).
115. Smajic J, Hafner C, Erni D. On the design of photonic crystal multiplexers. *Opt Express* **11**, 566–571 (2003).
116. Liu T, Zakharian AR, Fallahi M, Moloney JV, Mansuripur M. Multimode interference-based photonic crystal waveguide power splitter. *J Lightwave Technol* **22**, 2842–2846 (2004).
117. Hosseini A, Xu XC, Subbaraman H, Lin CY, Rahimi S et al. Large optical spectral range dispersion engineered silicon-based photonic crystal waveguide modulator. *Opt Express* **20**, 12318–12325 (2012).
118. Shi JX, Pollard ME, Angeles CA, Chen RQ, Gates JC et al. Photonic crystal and quasi-crystals providing simultaneous light coupling and beam splitting within a low refractive-index slab waveguide. *Sci Rep* **7**, 1812 (2017).
119. Balasaraswathi M, Singh M, Malhotra J, Dhasarathan V. A high-speed radio-over-free-space optics link using wavelength division multiplexing-mode division multiplexing-multibeam technique. *Comput Electr Eng* **87**, 106779 (2020).
120. Zhou ZL, Li EK, Zhang HG. Performance analysis of duobinary and AMI techniques using LG modes in hybrid MDM-WDM-FSO transmission system. *J Opt Commun* , 1–7 (2019).
121. Amphawan A, Fazea Y. Multidiameter optical ring and Hermite-Gaussian vortices for wavelength division multiplexing-mode division multiplexing. *Opt Eng* **55**, 106109 (2016).

122. Wang SP, Feng XL, Gao SM, Shi YC, Dai TG et al. On-chip reconfigurable optical add-drop multiplexer for hybrid wavelength/mode-division-multiplexing systems. *Opt Lett* **42**, 2802–2805 (2017).
123. Gao JT, Nazemosadat E, Yang Y, Fu SN, Tang M et al. Elliptical-core highly nonlinear few-mode fiber based OXC for WDM-MDM networks. *IEEE J Sel Top Quant Electron* **27**, 7600511 (2021).
124. Mulugeta T, Rasras M. Silicon hybrid (de)multiplexer enabling simultaneous mode and wavelength-division multiplexing. *Opt Express* **23**, 943–949 (2015).
125. Yang YD, Li Y, Huang YZ, Poon AW. Silicon nitride three-mode division multiplexing and wavelength-division multiplexing using asymmetrical directional couplers and microring resonators. *Opt Express* **22**, 22172–22183 (2014).
126. Nawwar OM, Shalaby HMH, Pokharel RK. Photonic crystal-based compact hybrid WDM/MDM (De)multiplexer for SOI platforms. *Opt Lett* **43**, 4176–4179 (2018).
127. He Y, Zhang Y, Wang HW, Sun L, Su YK. Design and experimental demonstration of a silicon multi-dimensional (de)multiplexer for wavelength-, mode- and polarization-division (de)multiplexing. *Opt Lett* **45**, 2846–2849 (2020).
128. Dai DX. Silicon-based multi-channel mode (de)multiplexer for on-chip optical interconnects. In *Proceedings of the Integrated Photonics Research*, *Silicon and Nanophotonics 2014* (Optica Publishing Group, 2014); http://doi.org/10.1364/IPRSN.2014.IM2A.2.
129. Wang J, Chen PX, Chen ST, Shi YC, Dai DX. Improved 8-channel silicon mode demultiplexer with grating polarizers. *Opt Express* **22**, 12799–12807 (2014).
130. Kakati D, Sonkar RK. A 2×320 Gbps hybrid PDM-MDM-OFDM system for high-speed terrestrial FSO communication. In *Proceedings of the 14th Pacific Rim Conference on Lasers and Electro-Optics (CLEO PR 2020)* C5F_3 (Optica Publishing Group, 2020); http://doi.org/10.1364/CLEOPR.2020.C5F_3.
131. Minz M, Mishra D, Sonkar RK, Khan MM. Grating-assisted MDM-PDM hybrid (de)multiplexer for optical interconnect applications. *Proc SPIE* **11193**, 111930C (2019).
132. Xu LH, Wang Y, El-Fiky E, Mao D, Kumar A et al. Compact broadband polarization beam splitter based on multimode interference coupler with internal photonic crystal for the SOI platform. *J Lightwave Technol* **37**, 1231–1240 (2019).
133. Wang Y, Ma ML, Yun H, Lu ZQ, Wang X et al. Ultra-compact sub-wavelength grating polarization splitter-rotator for silicon-on-insulator platform. *IEEE Photonics J* **8**, 7805709 (2016).
134. Sun CL, Yu Y, Ye MY, Chen GY, Zhang XL. An ultra-low crosstalk and broadband two-mode (de)multiplexer based on adiabatic couplers. *Sci Rep* **6**, 38494 (2016).
135. Lee SY, Darmawan S, Lee CW, Chin MK. Transformation between directional couplers and multi-mode interferometers based on ridge waveguides. *Opt Express* **12**, 3079–3085 (2004).
136. Chang WJ, Lu LLZ, Ren XS, Li DY, Pan ZP et al. Ultra-compact mode (de)multiplexer based on subwavelength asymmetric Y-junction. *Opt Express* **26**, 8162–8170 (2018).
137. Sun Y, Xiong YL, Winnie NY. Experimental demonstration of a two-mode (de)multiplexer based on a taper-etched directional coupler. *Opt Lett* **41**, 3743–3746 (2016).
138. Shalaby HMH. Bi-directional coupler as a mode-division multiplexer/demultiplexer. *J Lightwave Technol* **34**, 3633–3640 (2016).
139. Liu L. Densely packed waveguide array (DPWA) on a silicon chip for mode division multiplexing. *Opt Express* **23**, 12135–12143 (2015).
140. Yu ZJ, Tong YY, Tsang HK, Sun XK. High-dimensional communication on etchless lithium niobate platform with photonic bound states in the continuum. *Nat Commun* **11**, 2602 (2020).
141. Nguyen VH, Kim IK, Seok TJ. Silicon photonic mode-division reconfigurable optical add/drop multiplexers with mode-selective integrated MEMS switches. *Photonics* **7**, 80 (2020).
142. Wei YH, Zhang M, Dai DX. Multichannel mode-selective silicon photonic add/drop multiplexer with phase change material. *J Opt Soc Am B* **37**, 3341–3350 (2020).
143. González-Andrade D, Dias A, Wangüemert-Pérez JG, Ortega-Moñux A, Molina-Fernández Í et al. Experimental demonstration of a broadband mode converter and multiplexer based on subwavelength grating waveguides. *Opt Laser Technol* **129**, 106297 (2020).
144. Driscoll JB, Grote RR, Souhan B, Dadap JI, Lu M et al. Asymmetric Y junctions in silicon waveguides for on-chip mode-division multiplexing. *Opt Lett* **38**, 1854–1856 (2013).
145. Xing JJ, Li ZY, Xiao X, Yu JZ, Yu YD. Two-mode multiplexer and demultiplexer based on adiabatic couplers. *Opt Lett* **38**, 3468–3470 (2013).
146. Mehrabi K, Zarifkar A, Miri M. Silicon-based dual-mode polarization beam splitter for hybrid mode/polarization-division-multiplexed systems. *Opt Commun* **479**, 126474 (2021).
147. Manimaraboopathy M, Kumar GAS, Mohanraj J, Valliammai M. Realization of all-optical multiplexer-demultiplexer in mid-IR wavelengths using triple-core photonic quasi-crystal fiber. *Opt Commun* **481**, 126556 (2021).
148. Jiang WF, Cheng FY, Xu J, Wan HD. Compact and low-crosstalk mode (de)multiplexer using a triple plasmonic-dielectric waveguide-based directional coupler. *J Opt Soc Am B* **35**, 2532–2540 (2018).
149. Kaushalram A, Hegde G, Talabattula S. Mode hybridization analysis in thin film lithium niobate strip multimode waveguides. *Sci Rep* **10**, 16692 (2020).
150. Chen GFR, Choi JW, Sahin E, Ng DKT, Tan DTH. On-chip 1 by 8 coarse wavelength division multiplexer and multi-wavelength source on ultra-silicon-rich nitride. *Opt Express* **27**, 23549–23557 (2019).
151. Luo LW, Ophir N, Chen CP, Gabrielli LH, Poitras CB et al. WDM-compatible mode-division multiplexing on a silicon chip. *Nat Commun* **5**, 3069 (2014).
152. Han LS, Liang S, Xu JJ, Qiao LJ, Zhu HL et al. Simultaneous wavelength-and mode-division (de)multiplexing for high-capacity on-chip data transmission link. *IEEE Photonics J* **8**, 7903510 (2016).
153. Khonina SN, Kotlyar VV, Soifer VA. Self-reproduction of multimode hermite-gaussian beams. *Tech Phys Lett* **25**, 489–491 (1999).
154. Kotlyar VV, Soifer VA, Khonina SN. Rotation of multimode Gauss-Laguerre light beams in free space. *Tech Phys Lett* **23**, 657–658 (1997).
155. Kotlyar VV, Soifer VA, Khonina SN. Rotation of multimodal Gauss-Laguerre light beams in free space and in a fiber. *Opt Lasers Eng* **29**, 343–350 (1998).
156. Lyubopytov VS, Tlyavlin AZ, Sultanov AK, Bagmanov VK, Khonina SN et al. Mathematical model of completely optical

system for detection of mode propagation parameters in an optical fiber with few-mode operation for adaptive compensation of mode coupling. *Comput Opt* **37**, 352–359 (2013).
157. Kotlyar VV, Khonina SN, Soifer VA. Light field decomposition in angular harmonics by means of diffractive optics. *J Mod Opt* **45**, 1495–1506 (1998).
158. Khonina SN, Kotlyar VV, Soifer VA, Wang YX, Zhao DZ. Decomposition of a coherent light field using a phase Zernike filter. *Proc SPIE* **3573**, 550–553 (1998).
159. Khonina SN, Almazov AA. Design of multichannel phase spatial filter for selection of Gauss-Laguerre laser modes. *Proc SPIE* **4705**, 30–39 (2002).
160. Porfirev AP, Khonina SN. Experimental investigation of multi-order diffractive optical elements matched with two types of Zernike functions. *Proc SPIE* **9807**, 98070E (2016).
161. Khonina SN, Ustinov AV. Binary multi-order diffraction optical elements with variable fill factor for the formation and detection of optical vortices of arbitrary order. *Appl Opt* **58**, 8227–8236 (2019).
162. Khonina SN, Karpeev SV, Porfirev AP. Wavefront aberration sensor based on a multichannel diffractive optical element. *Sensors* **20**, 3850 (2020).
163. Khonina SN, Kotylar VV, Soifer VA. Diffraction computation of 'focusator' into longitudinal segment and multifocal lens. *Proc SPIE* **1780**, 17800J (1993).
164. Kotlyar VV, Khonina SN, Soifer VA. Iterative calculation of diffractive optical elements focusing into a three- dimensional domain and onto the surface of the body of rotation. *J Mod Opt* **43**, 1509–1524 (1996).
165. Kotlyar VV, Khonina SN, Soifer VA. Calculation of phase formers of non-diffracting images and a set of concentric rings. *Optik* **102**, 45–50 (1996).
166. Khonina SN, Kotlyar VV, Lushpin VV, Soifer VA. A method for design of composite DOEs for the generation of letter image. *Opt Mem Neutral Networks* **6**, 213–220 (1997).
167. Kotlyar VV, Khonina SN. Method for design of DOE for the generation of contour images. *Proc SPIE* **3348**, 48–55 (1998).
168. Porfirev AP, Khonina SN. Simple method for efficient reconfigurable optical vortex beam splitting. *Opt Express* **25**, 18722–18735 (2017).
169. Porfirev A, Khonina S, Azizian-Kalandaragh Y, Kirilenko M. Efficient generation of arrays of closed-packed high-quality light rings. *Photonics Nanostruct-Fundam Appl* **37**, 100736 (2019).
170. Porfirev AP, Khonina SN. Generation of closed-packed optical vortex beams using two-level pure-phase diffractive multiplexer. *AIP Conf Proc* **1874**, 040042 (2017).
171. Kudryashov SI, Danilov PA, Porfirev AP, Saraeva IN, Nguyen THT et al. High-throughput micropatterning of plasmonic surfaces by multiplexed femtosecond laser pulses for advanced IR-sensing applications. *Appl Surf Sci* **484**, 948–956 (2019).
172. Pavlov D, Gurbatov S, Kudryashov SI, Danilov PA, Porfirev AP et al. 10-million-elements-per-second printing of infrared-resonant plasmonic arrays by multiplexed laser pulses. *Opt Lett* **44**, 283–286 (2019).
173. Pavlov D, Porfirev A, Khonina S, Pan L, Kudryashov SI et al. Coaxial hole array fabricated by ultrafast femtosecond-laser processing with spatially multiplexed vortex beams for surface enhanced infrared absorption. *Appl Surf Sci* **541**, 148602 (2021).
174. Khonina SN, Kazanskiy NL, Khorin PA, Butt MA. Modern types of axicons: new functions and applications. *Sensors* **21**, 6690 (2021).
175. Wang F, Liu XL, Cai YJ. Propagation of partially coherent beam in turbulent atmosphere: a review (invited review). *Prog Electromagn Res* **150**, 123–143 (2015).
176. Korotkova O. *Random Light Beams*: *Theory and Applications* (CRC Press, Boca Raton, 2013).
177. Malik M, O'Sullivan M, Rodenburg B, Mirhosseini M, Leach J et al. Influence of atmospheric turbulence on optical communications using orbital angular momentum for encoding. *Opt Express* **20**, 13195–13200 (2012).
178. Eyyuboğlu HT. Propagation of higher order Bessel-Gaussian beams in turbulence. *Appl Phys B* **88**, 259–265 (2007).
179. Soifer V, Korotkova O, Khonina SN, Shchepakina E. Vortex beams in turbulent media: review. *Comput Opt* **40**, 605–624 (2016).
180. Porfirev AP, Kirilenko MS, Khonina SN, Skidanov RV, Soifer VA. Study of propagation of vortex beams in aerosol optical medium. *Appl Opt* **56**, E8–E15 (2017).
181. Zhou P, Wang XL, Ma YX, Ma HT, Xu XJ et al. Propagation property of a nonuniformly polarized beam array in turbulent atmosphere. *Appl Opt* **50**, 1234–1239 (2011).
182. Milione G, Nguyen TA, Leach J, Nolan DA, Alfano RR. Using the nonseparability of vector beams to encode information for optical communication. *Opt Lett* **40**, 4887–4890 (2015).
183. Khonina SN, Kotlyar VV, Soifer VA, Lautanen J, Honkanen M et al. Generating a couple of rotating nondiffracting beams using a binary-phase DOE. *Optik* **110**, 137–144 (1999).
184. Dubois F, Emplit P, Hugon O. Selective mode excitation in graded-index multimode fiber by a computer-generated optical mask. *Opt Lett* **19**, 433–435 (1994).
185. Karpeev SV, Pavelyev VS, Duparre M, Luedge B, Rockstuhl C et al. DOE-aided analysis and generation of transverse coherent light modes in a stepped-index optical fiber. *Opt Mem Neutral Networks (Inf Opt)* **12**, 27–34 (2003).
186. Khonina SN, Striletz AS, Kovalev AA, Kotlyar VV. Propagation of laser vortex beams in a parabolic optical fiber. *Proc SPIE* **7523**, 75230B (2010).
187. Ye JF, Li Y, Han YH, Deng D, Guo ZY et al. Excitation and separation of vortex modes in twisted air-core fiber. *Opt Express* **24**, 8310–8316 (2016).
188. Karpeev SV, Pavelyev VS, Khonina SN, Kazanskiy NL, Gavrilov AV et al. Fibre sensors based on transverse mode selection. *J Mod Opt* **54**, 833–844 (2007).
189. Khonina SN, Volotovsky SG. Self-reproduction of multimode laser fields in weakly guiding stepped-index fibers. *Opt Mem Neutral Networks* **16**, 167–177 (2007).
190. Karpeev S, Khonina SN. Experimental excitation and detection of angular harmonics in a step-index optical fiber. *Opt Mem Neutral Networks* **16**, 295–300 (2007).
191. Bozinovic N, Yue Y, Ren YX, Tur M, Kristensen P et al. Terabit-scale orbital angular momentum mode division multiplexing in fibers. *Science* **340**, 1545–1548 (2013).
192. Khonina SN, Karpeev SV, Paranin VD. A technique for simultaneous detection of individual vortex states of Laguerre-Gaussian beams transmitted through an aqueous suspension of microparticles. *Opt Lasers Eng* **105**, 68–74 (2018).
193. Moreno I, Davis JA, Ruiz I, Cottrell DM. Decomposition of radially and azimuthally polarized beams using a circular-polarization and vortex-sensing diffraction grating. *Opt Express* **18**,

7173–7183 (2010).
194. Khonina SN, Savelyev DA, Kazanskiy NL. Vortex phase elements as detectors of polarization state. *Opt Express* **23**, 17845–17859 (2015).
195. Fu SY, Zhang SK, Wang TL, Gao CQ. Rectilinear lattices of polarization vortices with various spatial polarization distributions. *Opt Express* **24**, 18486–18491 (2016).
196. Moreno I, Davis JA, Badham K, Sánchez-López MM, Holland JE et al. Vector beam polarization state spectrum analyzer. *Sci Rep* **7**, 2216 (2017).
197. Rosales-Guzmán C, Bhebhe N, Forbes A. Simultaneous generation of multiple vector beams on a single SLM. *Opt Express* **25**, 25697–25706 (2017).
198. Khonina SN, Porfirev AP, Karpeev SV. Recognition of polarization and phase states of light based on the interaction of non-uniformly polarized laser beams with singular phase structures. *Opt Express* **27**, 18484–18492 (2019).
199. Huang H, Xie GD, Yan Y, Ahmed N, Ren YX et al. 100 Tbit/s free-space data link enabled by three-dimensional multiplexing of orbital angular momentum, polarization, and wavelength. *Opt Lett* **39**, 197–200 (2014).
200. Zhu XM, Kahn JM. Free-space optical communication through atmospheric turbulence channels. *IEEE Trans Commun* **50**, 1293–1300 (2002).
201. Cai Y, Chen Y, Eyyuboğlu HT, Baykal Y. Propagation of laser array beams in a turbulent atmosphere. *Appl Phys B* **88**, 467–475 (2007).
202. Raddatz L, White IH, Cunningham DG, Nowell MC. An experimental and theoretical study of the offset launch technique for the enhancement of the bandwidth of multimode fiber links. *J Lightwave Technol* **16**, 324–331 (1998).
203. Sakaguchi J, Awaji Y, Wada N, Kanno A, Kawanishi T et al. Space division multiplexed transmission of 109-Tb/s data signals using homogeneous seven-core fiber. *J Lightwave Technol* **30**, 658–665 (2012).
204. Li SH, Wang J. A compact trench-assisted multi-orbital-angular-momentum multi-ring fiber for ultrahigh-density space-division multiplexing (19 rings × 22 modes). *Sci Rep* **4**, 3853 (2014).
205. Deng D, Li Y, Zhao H, Han YH, Ye J F et al. High-capacity spatial-division multiplexing with orbital angular momentum based on multi-ring fiber. *J Opt* **21**, 055601 (2019).

Acknowledgements

This work was financially supported by the Russian Foundation for Basic Research (grant No. 18-29-20045) for WDM, MDM and hybrid WDM-MDM, WDM-PDM sections, by the Russian Science Foundation (grant No. 21-79-20075) for PDM, OAMM and hybrid PDM-MDM sections, and by the Ministry of Science and Higher Education of the Russian Federation under the FSRC "Crystallography and Photonics" of the Russian Academy of Sciences (the state task No. 007-GZ/Ch3363/26) for comparative analysis.

Author contributions

We acknowledge the equal contribution of all the authors. S. N. Khonina- Investigation, data collection, review, and editing. N. L. Kazanskiy and S. V. Karpeev- Supervision and methodology. M. A. Butt-Original draft preparation, writing, review, and editing.

Competing interests

The authors declare no competing financial interests.